



ELSEVIER

Physica D 99 (1996) 81–107

PHYSICA D

Topology and dynamics in ferromagnetic media

S. Komineas, N. Papanicolaou *

Department of Physics, University of Crete, and Research Center of Crete, Heraklion, Greece

Received 17 November 1995; accepted 7 April 1996

Communicated by H. Flaschka

Abstract

A direct link between the topological complexity of ferromagnetic media and their dynamics has recently been established through the construction of unambiguous conservation laws as moments of a topological vorticity. In the present paper we carry out this program under completely realistic conditions, with due account of the long-range magnetostatic field and related boundary effects. In particular, we derive unambiguous expressions for the linear and angular momentum in a ferromagnetic film which are then used to study the dynamics of magnetic bubbles under the influence of an applied magnetic-field gradient. The semi-empirical golden rule of bubble dynamics is verified in its gross features but not in its finer details. A byproduct of our analysis is a set of virial theorems generalizing Derrick's scaling relation as well as a detailed recalculation of the fundamental magnetic bubble.

1. Introduction

Magnetic bubbles have been known to exhibit some distinct dynamical features due to their nontrivial topological structure. The inherent link between topology and dynamics was already apparent in the early work of Thiele [1] as well as in many investigations that followed [2,3]. The essence of the early work is best summarized by the experimentally observed skew deflection of magnetic bubbles under the influence of an applied magnetic-field gradient. The so-called golden rule of bubble dynamics relates the deflection angle δ to the winding number Q by

$$\frac{gr^2}{2V} \sin \delta = Q, \quad (1.1)$$

where g is the strength of the applied field gradient, r is the bubble radius and V its speed. This relation is

remarkable in two respects. First, it suggests that only topologically trivial ($Q = 0$) bubbles move in the direction of the gradient ($\delta = 0$), even though such a behavior would naively be expected for all magnetic bubbles; in fact, bubbles with a nonvanishing winding number ($Q = \pm 1, \pm 2, \dots$) tend to be deflected in a direction nearly perpendicular ($\delta \sim 90^\circ$) to the applied gradient. Second, Eq. (1.1) implies some sort of a topological quantization in that it relates the integer-valued winding number to experimentally measured quantities that can, in principle, assume any values.

Although the golden rule has been employed with considerable success in the analysis of actual experiments, especially for hard ($|Q| \gg 1$) bubbles, it is still a semi-empirical relation whose precise meaning and domain of validity must be specified. For instance, the meaning of the various quantities entering Eq. (1.1) needs to be explained because magnetic bubbles are extended structures rather than point-like

* Corresponding author. Fax: 30-81-394201

particles. Furthermore the usual derivations of (1.1) are based on the assumption that the bubble reaches a steady state, in the presence of dissipation, in which the deflection angle δ , the radius r and the speed V approach constant values. But such an assumption was never justified and is actually incorrect. In practice, experiments are analyzed by applying Eq. (1.1) with average values for the deflection angle and the speed and by assuming that the radius does not change significantly during the application of the gradient.

In some recent work on this subject [4] the link between topology and dynamics was made explicit through the construction of unambiguous conservation laws as moments of a suitable topological vorticity. The important qualitative features of bubble dynamics became then apparent. Thus, in the absence of external magnetic-field gradients or other perturbations, bubbles with a nonvanishing winding number cannot move freely but are always spontaneously pinned. On the other hand, in the absence of dissipation, a bubble would be deflected at a right angle ($\delta = 90^\circ$) with respect to an applied magnetic-field gradient, with a drift velocity that can be calculated analytically in some important special cases [4] and is generally consistent with Eq. (1.1). The emerging picture is analogous to the Hall motion of an electron as well as to the Magnus effect of fluid dynamics. These analogies further suggest that the deflection angle should deviate from 90° in the presence of dissipation. However an exact calculation of the deflection angle, i.e., a derivation of the golden rule, is no longer possible on the basis of conservation laws alone.

Therefore the semi-quantitative picture derived from the conservation laws must be supplemented by some results from a numerical solution of the underlying Landau–Lifshitz equation. Such a solution is not straightforward under completely realistic conditions; calculation of the long-range magnetostatic field is always a problem and the finite thickness of actual magnetic films forces one to work with a three-dimensional (3D) grid, even though the essential topological structure of magnetic bubbles is two-dimensional (2D). Hence our numerical efforts have thus far been restricted to strictly 2D models of increasing complexity [5,6].

It is the purpose of the present paper to provide a precise formulation within the quasi-2D geometry of realistic ferromagnetic films, taking into account the effects from the film boundaries and the magnetostatic field. In Section 2 we review some basic facts about the Landau–Lifshitz equation and introduce convenient (rationalized) physical units. In Section 3 we discuss the two ingredients that are important to establish a direct link between the topological complexity of magnetic structures and their dynamics, the gyrovector and the stress tensor. The derivation of unambiguous conservation laws is then carried out in Section 4 in the presence of film boundaries. A byproduct of our study of conservation laws is a set of virial theorems that generalize the well-known scaling relation of Derrick [7], an issue taken up in Section 5. A detailed numerical calculation of the fundamental ($Q = 1$) bubble is presented in Section 6 which is consistent with the virial theorems. The issue of skew deflection in an applied magnetic-field gradient is studied in Section 7 where we find that the semi-empirical golden rule is verified in its gross features but not in its details. Our conclusions are summarized in Section 8 together with some suggestions for further work.

2. Landau–Lifshitz equation

A ferromagnetic medium is described in terms of the density of magnetic moment or magnetization \mathbf{M} which is due primarily to the electron spin but may include contributions also from the orbital motion. In general, the vector $\mathbf{M} = (M_1, M_2, M_3)$ is a function of position and time except that its magnitude is nearly constant for a wide temperature range sufficiently below the Curie point:

$$\mathbf{M} = \mathbf{M}(x, t), \quad M^2 \equiv M_1^2 + M_2^2 + M_3^2 = M_0^2, \quad (2.1)$$

where $\mathbf{x} = (x_1, x_2, x_3)$ is the position vector, t is the time variable, and the constant M_0 is the saturation magnetization.

Static as well as dynamical properties of the magnetization are governed by the Landau–Lifshitz equation

$$\frac{\partial \mathbf{M}}{\partial t} + \gamma (\mathbf{M} \times \mathbf{F}) = \frac{\lambda}{M_0} \left(\mathbf{M} \times \frac{\partial \mathbf{M}}{\partial t} \right), \quad (2.2)$$

which describes precession around an effective field \mathbf{F} with the constant γ given by

$$\gamma = \frac{g_e |e|}{2m_e c}, \quad (2.3)$$

where $g_e \sim 2$ is the gyromagnetic ratio, e the electron charge, m_e the electron mass, and c the velocity of light. Eq. (2.2) also includes a phenomenological (Landau–Gilbert) dissipative term where the dissipation constant λ is dimensionless. This choice of dissipation preserves the magnitude of magnetization.

The effective field \mathbf{F} may be written as

$$\mathbf{F} = \mathbf{F}_e + \mathbf{F}_a + \mathbf{H}_b + \mathbf{H}. \quad (2.4)$$

Here \mathbf{F}_e is the exchange field

$$\mathbf{F}_e = \frac{2A}{M_0^2} \Delta \mathbf{M}, \quad (2.5)$$

where A is the exchange stiffness constant and Δ the Laplace operator. \mathbf{F}_a is the anisotropy field

$$\mathbf{F}_a = -\frac{2K}{M_0^2} (M_1, M_2, 0), \quad (2.6)$$

where K is a positive constant leading to an easy axis in the third direction. In ferromagnetic films made out of bubble materials the easy axis is perpendicular to the film surface [2]. \mathbf{H}_b is a uniform bias field,

$$\mathbf{H}_b = (0, 0, H_b), \quad H_b = \text{const}, \quad (2.7)$$

applied along the easy axis. Finally \mathbf{H} is the magnetic field produced by the magnetization itself and thus satisfies the magnetostatic equations

$$\nabla \times \mathbf{H} = 0, \quad \nabla \cdot \mathbf{B} = 0; \quad \mathbf{B} = \mathbf{H} + 4\pi \mathbf{M}, \quad (2.8)$$

where \mathbf{B} is the corresponding magnetic induction. The use of the magnetostatic instead of the complete Maxwell equations is justified by the fact that time variations of magnetic structures of practical interest are slow.

Numerical values of the various constants introduced above may be found in Ref. [2] for a number of

ferromagnetic materials. However using all these constants within a theoretical development clouds the underlying simplicity of the Landau–Lifshitz equation. Hence we introduce rationalized physical units as follows. First, we work with the normalized magnetization

$$\mathbf{m} = \mathbf{M}/M_0, \quad m^2 = 1. \quad (2.9)$$

Second, we measure distance, time and magnetic field (induction) in units of

$$\sqrt{\frac{A}{2\pi M_0^2}}, \quad \frac{1}{4\pi \gamma M_0}, \quad \text{and} \quad 4\pi M_0, \quad (2.10)$$

respectively. We further define the dimensionless anisotropy constant

$$\kappa = \frac{K}{2\pi M_0^2}, \quad (2.11)$$

which is usually referred to as the quality factor. Finally, we introduce new symbols for dimensionless magnetic fields such as $\mathbf{h} = \mathbf{H}/4\pi M_0$, but maintain the same symbols \mathbf{x} and t for the rationalized space and time variables.

The Landau–Lifshitz equation is then written as

$$\dot{\mathbf{m}} + (\mathbf{m} \times \mathbf{f}) = \lambda (\mathbf{m} \times \dot{\mathbf{m}}), \quad m^2 = 1, \quad (2.12)$$

where the dot denotes differentiation with respect to time, a convention that will be adopted from now on. The effective field \mathbf{f} is given by

$$\mathbf{f} = \Delta \mathbf{m} - \kappa (m_1, m_2, 0) + \mathbf{h}_b + \mathbf{h}, \quad (2.13)$$

where $\mathbf{h}_b = (0, 0, h_b)$ is the bias field and \mathbf{h} satisfies the magnetostatic equations

$$\nabla \times \mathbf{h} = 0, \quad \nabla \cdot \mathbf{b} = 0; \quad \mathbf{b} = \mathbf{h} + \mathbf{m}. \quad (2.14)$$

The only free parameters are now the quality factor κ , the dissipation constant λ , and the bias field h_b . One should add that Eq. (2.12) differs from the Landau–Lifshitz equation studied in our earlier work [4] by the overall replacement $\mathbf{m} \rightarrow -\mathbf{m}$ that originates in a sign difference between magnetization and spin introduced by the negative electron charge and is only a matter of convention. The resulting sign differences at various

stages of the calculation will be incorporated without further notice.

The remainder of this section is devoted to a discussion of the hamiltonian structure associated with the Landau–Lifshitz equation at vanishing dissipation ($\lambda = 0$). Then we write

$$\dot{\mathbf{m}} + (\mathbf{m} \times \mathbf{f}) = 0, \quad m^2 = 1, \quad (2.15)$$

where the effective field \mathbf{f} is still given by Eq. (2.13) and may be expressed entirely in terms of the magnetization once the magnetostatic field \mathbf{h} is determined by solving the linear system (2.14). Now a conserved energy functional $W = W(\mathbf{m})$ exists such that the effective field is obtained through the general relation

$$\mathbf{f} = -\frac{\delta W}{\delta \mathbf{m}}, \quad (2.16)$$

where the symbol δ denotes the usual functional derivative. Eq. (2.16) together with Eq. (2.15) imply that the functional W is indeed conserved, and that (2.15) is the Hamilton equation associated with the hamiltonian W endowed with the Poisson bracket relations

$$\{m_i(\mathbf{x}), m_j(\mathbf{x}')\} = \varepsilon_{ijk} m_k(\mathbf{x}) \delta(\mathbf{x} - \mathbf{x}'), \quad (2.17)$$

which are reminiscent of the spin commutation relations. Here ε_{ijk} is the 3D antisymmetric tensor and the usual summation convention for repeated indices is invoked.

In order to display the explicit form of the energy functional we write

$$W = W_e + W_a + W_b + W_m, \quad (2.18)$$

where the four terms correspond to the exchange, anisotropy, bias, and magnetostatic field. The more or less obvious choice of the exchange energy,

$$W_e = \int w_e dV, \quad w_e = \frac{1}{2} (\partial_i \mathbf{m} \cdot \partial_i \mathbf{m}), \quad (2.19)$$

where w_e is the corresponding energy density, requires some qualification in the presence of boundaries. Consider the functional variation

$$\begin{aligned} \delta W_e &= \int (\partial_i \delta \mathbf{m} \cdot \partial_i \mathbf{m}) dV \\ &= \oint (\delta \mathbf{m} \cdot \partial_i \mathbf{m}) dS_i - \int (\delta \mathbf{m} \cdot \Delta \mathbf{m}) dV, \end{aligned} \quad (2.20)$$

where the surface-element vector $d\mathbf{S} = (dS_1, dS_2, dS_3)$ is perpendicular to the boundaries of the ferromagnetic medium. Eq. (2.20) would yield the desired relation

$$\mathbf{F}_e = -\frac{\delta W_e}{\delta \mathbf{m}} = \Delta \mathbf{m} \quad (2.21)$$

if the surface integral were absent; that is, if the gradient of the magnetization along the normal to the surface vanished. We write symbolically

$$\frac{\partial \mathbf{m}}{\partial n} = 0, \quad (2.22)$$

which will be viewed as a boundary condition to be imposed at the free boundaries of the medium, in addition to the familiar boundary conditions of magnetostatics. This ‘‘unpinned’’ boundary condition was previously employed in the study of ferromagnetic films [2] and will play an important role in the following.

On the other hand, the usual bulk expressions for the anisotropy and bias (Zeeman) energies,

$$\begin{aligned} W_a &= \int w_a dV, \quad w_a = \frac{1}{2} \kappa (m_1^2 + m_2^2), \\ W_b &= \int w_b dV, \quad w_b = h_b (1 - m_3), \end{aligned} \quad (2.23)$$

are free of boundary ambiguities and obviously yield the corresponding contributions to the effective field through the general relation (2.16). Note that in the Zeeman energy we have subtracted the (trivial) contribution from the state

$$\mathbf{m}_0 = (0, 0, 1), \quad (2.24)$$

which describes a fully saturated ferromagnet and will thus be referred to as the ground state. Configuration (2.24) is the simplest example of a static solution of the Landau–Lifshitz equation.

Boundary effects are also important in the definition of the magnetostatic energy and will be described here in some detail. We begin with the reasonable ansatz

$$W_m = \frac{1}{2} \int \mathbf{h}^2 dV, \quad (2.25)$$

where it is understood that the integral extends over all volume, inside and outside the material, and that the field \mathbf{h} is expressed in terms of the magnetization through Eqs. (2.14). However, in order to justify

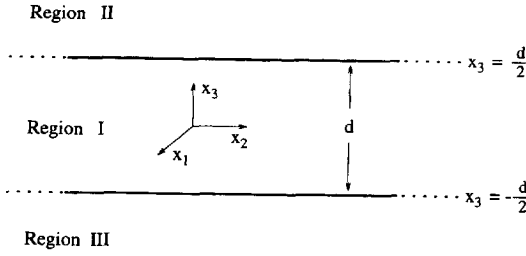


Fig. 1. Conventions concerning a ferromagnetic film of thickness d . The film extends to infinity in the x_1 and x_2 directions.

that (2.25) is an appropriate choice of the magnetostatic energy within the context of the Landau–Lifshitz equation, one must show that

$$\mathbf{h} = -\frac{\delta W_m}{\delta \mathbf{m}}. \quad (2.26)$$

Such a demonstration is not completely straightforward because of the implicit dependence of \mathbf{h} on the magnetization.

To make this dependence explicit we introduce a scalar potential ψ from

$$\mathbf{h} = -\nabla\psi, \quad \Delta\psi = (\nabla \cdot \mathbf{m}), \quad (2.27)$$

and solve the Poisson equation to obtain

$$\psi(\mathbf{x}) = \frac{1}{4\pi} \left[\oint \frac{\mathbf{m}(\mathbf{x}') \cdot d\mathbf{S}'}{|\mathbf{x} - \mathbf{x}'|} - \int \frac{(\nabla \cdot \mathbf{m})(\mathbf{x}')}{|\mathbf{x} - \mathbf{x}'|} dV' \right], \quad (2.28)$$

where the surface integral extends over the boundaries of the ferromagnetic medium, if any, and the volume integral over the bulk of the medium. Applying a careful partial integration yields the equivalent relation

$$\psi(\mathbf{x}) = \frac{1}{4\pi} \int \frac{(\mathbf{x} - \mathbf{x}') \cdot \mathbf{m}(\mathbf{x}')}{|\mathbf{x} - \mathbf{x}'|^3} dV', \quad (2.29)$$

whose advantage is that it contains no derivatives of the magnetization and is valid irrespectively of the presence of boundaries.

As an elementary illustration we consider a ferromagnetic film of thickness d (see Fig. 1) and assume that the magnetization is equal to its ground-state value (2.24) inside the film (region I) and vanishes outside (regions II and III). An explicit calculation of the integral in Eq. (2.29) then yields

$$\psi = \begin{cases} \frac{1}{2}d, & x_3 > \frac{1}{2}d \\ x_3, & -\frac{1}{2}d < x_3 < \frac{1}{2}d, \\ -\frac{1}{2}d, & x_3 < -\frac{1}{2}d. \end{cases} \quad (2.30)$$

Therefore the magnetic field is given by $\mathbf{h} = -\nabla\psi = -\mathbf{m}_0$ inside the film and vanishes outside. The magnetic induction $\mathbf{b} = \mathbf{h} + \mathbf{m}_0$ vanishes everywhere.

We now return to the magnetostatic energy (2.25) and replace \mathbf{h}^2 by $-\mathbf{h} \cdot (\nabla\psi)$. An application of the divergence theorem and Eqs. (2.14) then gives

$$W_m = \frac{1}{2} \left[\oint \psi(\mathbf{m} \cdot d\mathbf{S}) - \int \psi(\nabla \cdot \mathbf{m}) dV \right], \quad (2.31)$$

where we have also used the fact that ψ is continuous across the boundary and that the difference between the normal components of the magnetic field on the two sides of the boundary is equal to the normal component of the magnetization. A further partial integration transforms (2.31) into

$$W_m = -\frac{1}{2} \int (\mathbf{h} \cdot \mathbf{m}) dV, \quad (2.32)$$

which shares with Eq. (2.29) the property that it is valid whether or not boundaries are present. Hence, using this form of the magnetostatic energy and a magnetic field calculated from Eq. (2.29), the basic relation (2.26) is established by straightforward manipulations.

We complete the discussion of the canonical structure noting that the Landau–Lifshitz equation is actually a constrained hamiltonian system. Nevertheless one may resolve the constraint $\mathbf{m}^2 = 1$ explicitly using, for example, the spherical parametrization

$$\begin{aligned} m_1 &= \sin \Theta \cos \Phi, \\ m_2 &= \sin \Theta \sin \Phi, \quad m_3 = \cos \Theta. \end{aligned} \quad (2.33)$$

The energy functional is then parametrized in terms of the two independent fields Θ and Φ and the general form of the Landau–Lifshitz equation reads

$$\sin \Theta \dot{\Theta} = -\frac{\delta W}{\delta \Phi}, \quad \sin \Theta \dot{\Phi} = \frac{\delta W}{\delta \Theta}, \quad (2.34)$$

which suggests that the pair of fields

$$\Pi = \cos \Theta \quad \text{and} \quad \Phi \quad (2.35)$$

is a canonical pair:

$$\dot{\Pi} = \frac{\delta W}{\delta \Phi}, \quad \dot{\Phi} = -\frac{\delta W}{\delta \Pi}. \quad (2.36)$$

However most of the special dynamical features of the ferromagnetic continuum emerge exactly when the definition of the canonical variables (2.35) encounters ambiguities due to a possibly nontrivial topological structure of the magnetization.

Finally we return briefly to the issue of dissipation and rewrite Eq. (2.12) in the equivalent form

$$\begin{aligned} \dot{\mathbf{m}} + (\mathbf{m} \times \mathbf{G}) &= 0, \quad \mathbf{m}^2 = 1, \\ \mathbf{G} &= \lambda_1 \mathbf{f} + \lambda_2 (\mathbf{m} \times \mathbf{f}), \\ \lambda_1 &= \frac{1}{1 + \lambda^2}, \quad \lambda_2 = \frac{\lambda}{1 + \lambda^2}. \end{aligned} \quad (2.37)$$

We then examine the rate at which the energy changes in the presence of dissipation:

$$\begin{aligned} \dot{W} &= \int \left(\frac{\delta W}{\delta \mathbf{m}} \cdot \dot{\mathbf{m}} \right) dV \\ &= -\lambda_2 \int [f^2 - (\mathbf{m} \cdot \mathbf{f})^2] dV. \end{aligned} \quad (2.38)$$

Because \mathbf{m} is a unit vector the integrand in the last step of Eq. (2.38) is positive definite and the energy decreases when the dissipation constant λ is positive.

3. Gyrovector and the stress tensor

The key quantity for the description of both topological and dynamical properties of the magnetization is the gyrovector or vorticity $\gamma = (\gamma_1, \gamma_2, \gamma_3)$ whose cartesian components are given by

$$\gamma_i = -\frac{1}{2} \varepsilon_{ijk} (\partial_j \mathbf{m} \times \partial_k \mathbf{m}) \cdot \mathbf{m}. \quad (3.1)$$

The former terminology was introduced in the early work [1] but the latter seems more appropriate in view of the significant formal analogy of the vector γ with ordinary vorticity in fluid dynamics. Nevertheless one should stress that γ is not related to actual rotational motion in the ferromagnetic continuum but rather to the topological complexity of the magnetization. For the moment, we are concerned with instantaneous properties of the unit vector field $\mathbf{m} =$

$\mathbf{m}(\mathbf{x})$ at some instant t that is not displayed explicitly. Questions of dynamics will be addressed later in this section.

An immediate consequence of the definition (3.1) and the constraint $\mathbf{m}^2 = 1$ is that the vorticity field is solenoidal,

$$\nabla \cdot \gamma = 0, \quad (3.2)$$

and hence the corresponding vortex lines cannot terminate but at the boundaries of the ferromagnetic medium. The precise nature of vortex lines is revealed by expressing the vorticity in terms of the canonical variables (2.35),

$$\gamma = \nabla \Pi \times \nabla \Phi, \quad (3.3)$$

a relation that suggests an analogy of Π and Φ with the Clebsch potentials of fluid dynamics [8]. It also establishes that vortex lines are defined as the intersections of the two surfaces $\Pi(\mathbf{x}) = c_1$ and $\Phi(\mathbf{x}) = c_2$ where c_1 and c_2 are arbitrary constants. In other words, vortex lines are the curves along which the magnetization vector \mathbf{m} remains constant.

Such a simple definition of vortex lines allows a transparent topological classification of the possible distributions of magnetization. We shall consider the physically interesting class of configurations $\mathbf{m} = \mathbf{m}(\mathbf{x})$ that are differentiable functions of position and approach the ground state of the ferromagnet at spatial infinity:

$$\mathbf{m}(\mathbf{x}) \xrightarrow{|\mathbf{x}| \rightarrow \infty} \mathbf{m}_0 = (0, 0, 1). \quad (3.4)$$

In the absence of boundaries the medium extends to infinity in all directions and vortex lines are closed curves. One may then define a degree of knottedness, or helicity, of tangled vortex lines by analogy with related work in fluid dynamics [9] and magneto-hydrodynamics [10]. The current status of the topological aspects of the above subjects may be traced from Ref. [11]. In the present context, such a degree is more appropriately referred to as the Hopf index [12]. In view of the boundary condition (3.4) the 3D space is isomorphic to the sphere S^3 and a specific configuration $\mathbf{m} = \mathbf{m}(\mathbf{x})$ establishes a map from S^3 to S^2 , where S^2 is the 2D sphere defined from the constraint

$m^2 = 1$. Such a map is characterized by the integer-valued Hopf index defined as follows. Let $\mathbf{m}(\mathbf{x}) = \mathbf{m}_1$ and $\mathbf{m}(\mathbf{x}) = \mathbf{m}_2$ be any two vortex lines where \mathbf{m}_1 and \mathbf{m}_2 are constant unit vectors. The linking number of these two curves is independent of the specific choice of the pair of vortex lines and is called the Hopf index of configuration $\mathbf{m}(\mathbf{x})$.

In order to make a first contact with the dynamics we also quote an analytical definition of the Hopf index. The solenoidal vorticity is derived from a vector potential \mathbf{a} ,

$$\boldsymbol{\gamma} = \nabla \times \mathbf{a}, \quad (3.5)$$

and the Hopf index is given by

$$N = \frac{1}{4\pi} \int (\mathbf{a} \cdot \boldsymbol{\gamma}) dV. \quad (3.6)$$

Although the vector potential is unique only to within a gauge transformation, N is gauge invariant and may be expressed entirely in terms of $\boldsymbol{\gamma}$ by

$$N = \frac{1}{(4\pi)^2} \int \varepsilon_{ijk} \gamma_i(\mathbf{x}) \frac{(\mathbf{x} - \mathbf{x}')_j}{|\mathbf{x} - \mathbf{x}'|^3} \gamma_k(\mathbf{x}') dV dV'. \quad (3.7)$$

The remarkable fact is that the above integral is always equal to an integer and its explicit values coincide with those obtained through the linking-number definition given in the preceding paragraph [13,14].

It would appear that a simpler (local) expression for the vector potential may be derived from Eq. (3.3) which suggests that

$$\mathbf{a} = \Pi \nabla \Phi, \quad (3.8)$$

provided that Π and Φ are differentiable functions of position. However inserting (3.3) and (3.8) in (3.6) would then lead to a vanishing Hopf index. Putting it differently, the canonical variables Π and Φ cannot be both differentiable for field configurations with $N \neq 0$, even though the magnetization is always assumed to be differentiable. Indeed, explicit examples worked out in the literature [4,15] demonstrate that the magnetization reaches the north as well as the south pole of the sphere $m^2 = 1$ along certain (vortex) lines where the angular variable Φ becomes multivalued

when $N \neq 0$. While these difficulties are largely irrelevant, because of the gauge-invariant definition (3.7), they already provide an important hint concerning dynamics. Note that the vector potential (3.8) coincides with the familiar expression for the momentum density associated with the Hamilton equations (2.36). We thus conclude that the difficulties discussed in connection with Eq. (3.8) render ambiguous also the usual linear momentum.

We defer for the moment further discussion of dynamics and return to the question of topological classification in the presence of boundaries. Specifically we consider the film geometry of Fig. 1 where vortex lines need not be closed but may terminate at the boundaries of the film. Hence a definition of a Hopf index is no longer meaningful. Instead we consider the flux of vorticity

$$Q = \frac{1}{4\pi} \int_S \boldsymbol{\gamma} \cdot d\mathbf{S} \quad (3.9)$$

through any open surface S that is contained within the film but extends to infinity on all sides. The flux is independent of the specific choice of a surface with the above properties, thanks to $\nabla \cdot \boldsymbol{\gamma} = 0$ and an elementary application of the divergence theorem. In particular, S may be a plane perpendicular to the third axis,

$$Q = \frac{1}{4\pi} \int \gamma_3 dx_1 dx_2, \quad -\frac{1}{2}d < x_3 < \frac{1}{2}d, \quad (3.10)$$

where the double integral is independent of x_3 . In fact, this integral coincides with the Pontryagin index or winding number [13] of the magnetization and is also integer-valued ($Q = 0, \pm 1, \pm 2, \dots$). Again, when $Q \neq 0$, the canonical variables Π and Φ cannot be defined everywhere and the corresponding linear momentum is ambiguous.

The topological classification described above does not assume that the configuration $\mathbf{m} = \mathbf{m}(\mathbf{x})$ solves the Landau–Lifshitz equation but merely that it obeys some general physical restrictions such as differentiability and Eq. (3.4). Of course, this classification would become especially relevant if stationary solutions were found with a nontrivial topology. In this respect, we note that arguments of varying completeness

have been presented in the literature for the existence of magnetic vortex rings with a nonvanishing Hopf index [4,15] but a definite theoretical treatment and actual observation are still lacking. Nonetheless magnetic bubbles with a wide range of winding numbers have been observed in ferromagnetic films [2,3]. Finally, if the magnetization itself is allowed to be non-differentiable at isolated singular points, one is naturally led to a class of topological *defects* that are also characterized by a winding number of the form (3.9) except that the surface S is closed around a singular point. Such defects have been observed in the bulk of the ferromagnetic continuum and are called Bloch points [2,3].

We now organize the various hints concerning the connection between topology and dynamics by considering the time evolution of the vorticity (3.1). An elementary calculation based on the Landau–Lifshitz equation at vanishing dissipation, Eq. (2.15), leads to

$$\dot{\gamma}_i = -\varepsilon_{ijk} \partial_j (\mathbf{f} \cdot \partial_k \mathbf{m}) = \varepsilon_{ijk} \partial_j \tau_k, \quad (3.11)$$

where

$$\tau_k \equiv -(\mathbf{f} \cdot \partial_k \mathbf{m}) = \left(\frac{\delta W}{\delta \mathbf{m}} \cdot \partial_k \mathbf{m} \right) \quad (3.12)$$

is the “generalized force density” that appeared first in the work of Thiele [1]. We take this calculation one step farther using the formal argument

$$\int \tau_k dV = \int \left(\frac{\delta W}{\delta \mathbf{m}} \cdot \partial_k \mathbf{m} \right) dV = \partial_k W = 0 \quad (3.13)$$

to conclude that τ_k may be written as a total divergence,

$$\tau_k = \partial_l \sigma_{kl}, \quad (3.14)$$

where σ_{kl} will be called the stress tensor. Eq. (3.11) then reads

$$\dot{\gamma}_i = \varepsilon_{ijk} \partial_j \partial_l \sigma_{kl} \quad (3.15)$$

and proves to be fundamental for our purposes [4].

To complete this line of reasoning we must also supply an explicit expression for the stress tensor. As a first step we insert in Eq. (3.12) the effective field \mathbf{f} of Eq. (2.13):

$$\begin{aligned} \tau_k &= \tau_k^e + \tau_k^a + \tau_k^b + \tau_k^m, \\ \tau_k^e &= -(\Delta \mathbf{m} \cdot \partial_k \mathbf{m}), \\ \tau_k^a &= \kappa (m_1 \partial_k m_1 + m_2 \partial_k m_2), \\ \tau_k^b &= -h_b \partial_k m_3, \\ \tau_k^m &= -(\mathbf{h} \cdot \partial_k \mathbf{m}). \end{aligned} \quad (3.16)$$

We then search for a tensor

$$\sigma_{kl} = \sigma_{kl}^e + \sigma_{kl}^a + \sigma_{kl}^b + \sigma_{kl}^m \quad (3.17)$$

that must lead to Eq. (3.16) by applying the general relation (3.14). The first three terms are simply

$$\begin{aligned} \sigma_{kl}^e &= w_e \delta_{kl} - (\partial_k \mathbf{m} \cdot \partial_l \mathbf{m}), \\ \sigma_{kl}^a &= w_a \delta_{kl}, \quad \sigma_{kl}^b = w_b \delta_{kl}, \end{aligned} \quad (3.18)$$

where w_e , w_a and w_b are the energy densities defined in Eqs. (2.19) and (2.23). The construction of the magnetostatic contribution is slightly more involved but trial and error leads to

$$\sigma_{kl}^m = h_k b_l - \frac{1}{2} \mathbf{b}^2 \delta_{kl}, \quad (3.19)$$

where the magnetic induction $\mathbf{b} = \mathbf{h} + \mathbf{m}$ is used mostly as a notational abbreviation. As usual, it is understood that the magnetic field in Eq. (3.19) is expressed in terms of the magnetization through the magnetostatic equations (2.14). A repeated application of these equations establishes the desired relation

$$\partial_l \sigma_{kl}^m = -(\mathbf{h} \cdot \partial_k \mathbf{m}) = \tau_k^m. \quad (3.20)$$

A notable feature of the derived stress tensor σ_{kl} is that all but the magnetostatic contributions are symmetric under exchange of the indices k and l . The asymmetry of the last term anticipates the physical fact that the orbital angular momentum and the total magnetization are not separately conserved in the presence of the magnetostatic interaction, as we shall see shortly. A further interesting property is that the preceding construction applies whether or not boundaries are present, taking into account that the magnetic induction \mathbf{b} is equal to the magnetic field \mathbf{h} outside the ferromagnetic material where the stress tensor reduces to

$$\sigma_{kl} = \sigma_{kl}^m = h_k h_l - \frac{1}{2} \mathbf{h}^2 \delta_{kl}, \quad (3.21)$$

which is symmetric and satisfies the continuity equation

$$\partial_l \sigma_{kl} = 0 \quad (3.22)$$

by virtue of $\nabla \times \mathbf{h} = 0 = \nabla \cdot \mathbf{h}$. Eq. (3.22) is consistent with a vanishing Thiele force density outside the material.

4. Conservation laws

The occurrence of ambiguities in the canonical definition of conservation laws has already received considerable attention. Slonczweski [16] was apparently the first to recognize that the usual definition of linear momentum fails for magnetic bubbles with a nonvanishing winding number. Haldane [17] and Volovik [18] also addressed the question from different perspectives. But we believe that a simple as well as complete resolution of this issue was given only in some recent work [4] where the linear and angular momentum were expressed as moments of the topological vorticity (3.1). Since the available studies address strictly 2D or 3D models, our aim here is to establish unambiguous conservation laws in the context of the quasi-2D geometry appropriate for the description of ferromagnetic films.

We consider the geometry of Fig. 1 where a film of constant thickness d extends to infinity in the (x_1, x_2) plane and the easy axis is perpendicular to the film. Therefore the relevant symmetries are: (i) translations in the (x_1, x_2) plane, and (ii) azimuthal rotations around the third axis. We shall show that the corresponding conserved quantities are the moments

$$I_\mu = \int x_\mu \gamma_3 dV, \quad \mu = 1 \text{ or } 2, \quad (4.1)$$

which are related to the linear momentum, and the third component of the total angular momentum

$$J = l + \mu;$$

$$l = \frac{1}{2} \int \rho^2 \gamma_3 dV, \quad \mu = \int (m_3 - 1) dV, \quad (4.2)$$

where $\rho^2 = x_1^2 + x_2^2$ and hence the ‘‘orbital’’ angular momentum l is also expressed as a moment of the vorticity; μ is the total magnetic moment along the easy axis, except that we have subtracted the trivial contribution from the ground state so that μ is finite and negative. It should be noted that all volume integrals in Eqs. (4.1) and (4.2) extend over region I of Fig. 1.

Although the conservation laws quoted above have a similar appearance with those derived for strictly 2D models [4] a proof of their validity is not obvious because of potential boundary effects. We consider first the time evolution of the moments (4.1),

$$\dot{I}_\mu = \int x_\mu \dot{\gamma}_3 dV = \varepsilon_{3jk} \int x_\mu \partial_j \partial_l \sigma_{kl} dV, \quad (4.3)$$

where we have used the fundamental relation (3.15) applied for $i = 3$. Notation is organized by asserting that Greek indices μ, ν, \dots assume only the two distinct values 1 and 2, corresponding to the two spatial coordinates x_1 and x_2 , while Latin indices i, j, \dots assume all three values, as usual. We further introduce the 2D antisymmetric tensor $\varepsilon_{\mu\nu}$, whose elements are $\varepsilon_{11} = 0 = \varepsilon_{22}$ and $\varepsilon_{12} = 1 = -\varepsilon_{21}$, and invoke the summation convention for repeated indices without exception. Then

$$\begin{aligned} \dot{I}_\mu &= \varepsilon_{\nu\lambda} \int x_\mu \partial_\nu \partial_l \sigma_{\lambda l} dV \\ &= \varepsilon_{\nu\lambda} \int [\partial_\nu (x_\mu \partial_l \sigma_{\lambda l}) - \delta_{\mu\nu} \partial_l \sigma_{\lambda l}] dV, \end{aligned} \quad (4.4)$$

where both terms in the integrand are in the form of a total divergence. Since the film extends to infinity in the x_1 and x_2 directions, the first integral vanishes for either $\nu = 1$ or 2 provided that the magnetization exhibits a reasonable behavior at large x_1 or x_2 . By reasonable we mean that the magnetization approaches its ground-state value sufficiently fast so that the energy of the configuration is finite. Then we may write

$$\dot{I}_\mu = -\varepsilon_{\mu\lambda} \int \partial_l \sigma_{\lambda l} dV, \quad (4.5)$$

where the integrand is also a total divergence but the integral need not vanish because the Latin index l is summed over all three values, $l = 1, 2$ and 3 , and

may lead to a nonvanishing contribution from the film boundaries, namely

$$\dot{I}_\mu = -\varepsilon_{\mu\lambda} \left[\int_{x_3=d/2} \sigma_{\lambda 3} dx_1 dx_2 - \int_{x_3=-d/2} \sigma_{\lambda 3} dx_1 dx_2 \right], \quad (4.6)$$

where the tensor elements $\sigma_{\lambda 3}$ are evaluated right inside the boundaries and are certainly not equal to zero.

However we may now return to the explicit form of the stress tensor given in Section 3 and apply it for $\sigma_{\lambda 3}$ with $\lambda \neq 3$ to obtain

$$\sigma_{\lambda 3} = -(\partial_\lambda \mathbf{m} \cdot \partial_3 \mathbf{m}) + h_\lambda b_3, \quad (4.7)$$

which must be evaluated at the boundaries of the film where $\partial_3 \mathbf{m} = 0$ on account of the unpinned boundary condition (2.22). Hence

$$\sigma_{\lambda 3}(x_1, x_2, x_3 = \pm \frac{1}{2} d) = h_\lambda b_3, \quad (4.8)$$

where we further note that the combination of fields $h_\lambda b_3$, with $\lambda = 1$ or 2 , is continuous across the boundaries thanks to the familiar boundary conditions of magnetostatics. The double integrals in Eq. (4.6) may thus be evaluated right outside the boundaries where the stress tensor satisfies the continuity equation (3.22). An application of the divergence theorem in region II yields

$$0 = \int_{\text{II}} \partial_l \sigma_{\lambda l} dV = - \int_{x_3=d/2} \sigma_{\lambda 3} dx_1 dx_2, \quad (4.9)$$

and a similar relation for region III. The net conclusion is that both integrals in Eq. (4.6) vanish and

$$\dot{I}_\mu = 0, \quad (4.10)$$

which is the desired result. We shall defer discussion of the interesting physical consequences of Eq. (4.10) until a corresponding result is obtained for the angular momentum.

The time evolution of the orbital angular momentum is governed again by the fundamental relation (3.15). The analog of Eq. (4.4) now reads

$$\begin{aligned} \dot{i} &= \frac{1}{2} \varepsilon_{\nu\lambda} \int \rho^2 \partial_\nu \partial_l \sigma_{\lambda l} dV \\ &= \frac{1}{2} \varepsilon_{\nu\lambda} \int [\partial_\nu (\rho^2 \partial_l \sigma_{\lambda l}) - 2x_\nu \partial_l \sigma_{\lambda l}] dV, \end{aligned} \quad (4.11)$$

where the first integral in the last step of Eq. (4.11) vanishes for both $\nu = 1$ and 2 :

$$\begin{aligned} \dot{i} &= -\varepsilon_{\nu\lambda} \int x_\nu \partial_l \sigma_{\lambda l} dV \\ &= \varepsilon_{\nu\lambda} \int [\sigma_{\lambda\nu} - \partial_l (x_\nu \sigma_{\lambda l})] dV. \end{aligned} \quad (4.12)$$

Recalling that the volume integration extends over region I we write

$$\begin{aligned} \int_{\text{I}} \partial_l (x_\nu \sigma_{\lambda l}) dV &= \int_{x_3=d/2} x_\nu \sigma_{\lambda 3} dx_1 dx_2 \\ &\quad - \int_{x_3=-d/2} x_\nu \sigma_{\lambda 3} dx_1 dx_2, \end{aligned} \quad (4.13)$$

where the double integrals may be calculated either above or below the film surfaces because the tensor elements $\sigma_{\lambda 3}$ given by Eq. (4.8) are continuous across the boundaries. An argument similar to that used in Eq. (4.9) then leads to

$$\int_{x_3=d/2} x_\nu \sigma_{\lambda 3} dx_1 dx_2 = - \int_{\text{II}} \sigma_{\lambda\nu} dV, \quad (4.14)$$

and

$$\int_{x_3=-d/2} x_\nu \sigma_{\lambda 3} dx_1 dx_2 = \int_{\text{III}} \sigma_{\lambda\nu} dV. \quad (4.15)$$

Therefore Eq. (4.13) may be rewritten as

$$\int_{\text{I}} \partial_l (x_\nu \sigma_{\lambda l}) dV = - \int_{\text{II}} \sigma_{\lambda\nu} dV - \int_{\text{III}} \sigma_{\lambda\nu} dV, \quad (4.16)$$

where the right-hand side is symmetric under exchange of the indices ν and λ because the stress tensor is symmetric outside the film. Hence inserting Eq. (4.16) in Eq. (4.12) yields a vanishing contribution, because of the contraction with the antisymmetric tensor $\varepsilon_{\nu\lambda}$, and

$$\dot{i} = \int_{\text{I}} \varepsilon_{\nu\lambda} \sigma_{\lambda\nu} dV. \quad (4.17)$$

To summarize, if the magnetostatic interaction were absent, the stress tensor would be symmetric in all regions and Eq. (4.17) would lead to a conserved orbital angular momentum ($\dot{l} = 0$). In general, using the complete stress tensor given in Eqs. (3.18) and (3.19),

$$\varepsilon_{\nu\lambda}\sigma_{\lambda\nu} = \varepsilon_{\nu\lambda}h_{\lambda}b_{\nu} = \varepsilon_{\nu\lambda}h_{\lambda}m_{\nu}, \quad (4.18)$$

and

$$\dot{l} = \int (m_1h_2 - m_2h_1) dV, \quad (4.19)$$

so that the orbital angular momentum is not by itself conserved.

Nevertheless a conservation law is obtained by including the total magnetic moment μ of Eq. (4.2) whose time derivative is computed by applying directly the Landau–Lifshitz equation (2.15) to write

$$\dot{\mu} = \int m_3 dV = - \int (\mathbf{m} \times \mathbf{f})_3 dV. \quad (4.20)$$

Now taking into account the explicit expression for the effective field \mathbf{f} of Eq. (2.13) we find that the contributions from the anisotropy and bias fields drop out of Eq. (4.20) and

$$\dot{\mu} = - \int (\mathbf{m} \times \Delta\mathbf{m} + \mathbf{m} \times \mathbf{h})_3 dV. \quad (4.21)$$

To compute the exchange contribution we note that

$$\begin{aligned} \int (\mathbf{m} \times \Delta\mathbf{m}) dV &= \int \partial_i (\mathbf{m} \times \partial_i \mathbf{m}) dV \\ &= \oint (\mathbf{m} \times \partial_i \mathbf{m}) dS_i, \end{aligned} \quad (4.22)$$

where the surface integral vanishes because of the unpinned boundary condition (2.22). Therefore

$$\dot{\mu} = - \int (\mathbf{m} \times \mathbf{h})_3 dV = - \int (m_1h_2 - m_2h_1) dV. \quad (4.23)$$

Comparing this result with Eq. (4.19) establishes that

$$\dot{j} = 0, \quad (4.24)$$

or that the total angular momentum $J = l + \mu$ is conserved.

Having thus demonstrated the validity of the conservation laws (4.1) and (4.2) we now turn to the

discussion of their physical content. We first note that these conservation laws are free of all ambiguities even for configurations with a nontrivial topological structure. Suffice it to say that the potential nondifferentiability of the canonical variables Π and Φ does not affect Eqs. (4.1) and (4.2) because they are both expressed in terms of the vorticity which can be calculated directly from the magnetization through Eq. (3.1). A detailed discussion of this issue may be found in our earlier work within a strictly 2D context [4] and applies here with minor modifications. Hence we will simply list the important points adapted to the present quasi-2D situation.

The conserved moments (4.1) are related to the linear momentum $\mathbf{p} = (p_1, p_2)$ by

$$p_{\mu} = \varepsilon_{\mu\nu}I_{\nu}, \quad \{p_{\mu}, \mathbf{m}\} = -\partial_{\mu}\mathbf{m}, \quad (4.25)$$

where the Poisson bracket relation establishes that \mathbf{p} is indeed the generator of translations in the (x_1, x_2) plane. However \mathbf{p} cannot be interpreted as ordinary momentum for two related reasons. First, the Poisson bracket of its two components,

$$\{p_1, p_2\} = -4\pi dQ, \quad (4.26)$$

does not vanish except for a vanishing winding number. Second, under translations in the plane, $x_1 \rightarrow x_1 + c_1$ and $x_2 \rightarrow x_2 + c_2$, the moments transform according to

$$I_{\mu} \rightarrow I_{\mu} + 4\pi dQc_{\mu}, \quad (4.27)$$

which is a consequence of definition (4.1) and Eq. (3.10). The nontrivial transformation of the linear momentum (4.25) implied by Eq. (4.27) is surely an unusual property because one would expect the momentum to remain unchanged under a rigid translation. Nevertheless the above properties suggest a formal analogy with the familiar electron motion in a uniform magnetic field, the role of the latter being played here by the winding number.

Therefore, when $Q \neq 0$, a more useful interpretation of the conserved moments is obtained through the guiding center coordinates

$$R_{\mu} = \frac{\int x_{\mu} \gamma_3 dV}{\int \gamma_3 dV} = \frac{I_{\mu}}{4\pi dQ}, \quad \mu = 1 \text{ or } 2, \quad (4.28)$$

which are conserved and transform as $(R_1, R_2) \rightarrow (R_1 + c_1, R_2 + c_2)$ under a rigid translation in the plane $(x_1, x_2) \rightarrow (x_1 + c_1, x_2 + c_2)$. The latter property suggests that the 2D vector $\mathbf{R} = (R_1, R_2)$ may be interpreted as the mean position of a magnetic bubble with $Q \neq 0$ in a ferromagnetic film, and its conservation implies that such a bubble cannot be found in a free translational motion. In other words, $Q \neq 0$ bubbles are always spontaneously pinned or frozen within the ferromagnetic medium provided that external perturbations are absent; in analogy with the electrons undergoing a 2D cyclotron motion in a uniform magnetic film, in the absence of electric fields.

The physical meaning of the orbital angular momentum l defined in Eq. (4.2) is also unusual, for it actually provides a measure of the size of a configuration with $Q \neq 0$. More precisely, one may define a mean squared radius from

$$r^2 = \frac{\int [(x_1 - R_1)^2 + (x_2 - R_2)^2] \gamma_3 dV}{\int \gamma_3 dV} = \frac{l}{2\pi dQ} - \mathbf{R}^2, \quad (4.29)$$

which is directly proportional to l when the latter is defined with respect to the guiding center ($\mathbf{R} = 0$). Note that we use the abbreviated 2D notation $\mathbf{R} = (R_1, R_2)$ and $\mathbf{R}^2 = R_1^2 + R_2^2$. The radius r of Eq. (4.29) plays an important role in our theoretical development but does not, in general, coincide with the native radius at which the third component of the magnetization vanishes ($m_3 = 0$). One should add that r would be a conserved quantity in the absence of the magneto-static interaction because the orbital angular momentum would then be by itself conserved.

In order to pursue further a meaningful discussion of dynamics, one must first ascertain the existence of interesting static solutions of the Landau–Lifshitz equation such as magnetic bubbles with a nonvanishing winding number; an issue addressed in the following two sections. We shall return to a more detailed study of the implications of the derived conservation laws for dynamics in Section 7.

5. Virial theorems

A simple scaling argument due to Derrick [7] leads to a virial relation that must be satisfied by any finite-energy static solution of a nonlinear field theory. Since Derrick's relation is mainly used in the literature to establish the nonexistence of nontrivial static solutions, it is of some interest to demonstrate how the present theory evades its potential consequences and leads to the observed wealth of magnetic bubbles with practically any winding number [2]. However a generalization of the original scaling argument to the present case is not completely straightforward, because of the film boundaries, and is given below.

Static solutions are stationary points of the energy functional $W = W(\mathbf{m})$ provided that the constraint $\mathbf{m}^2 = 1$ is taken into account. For instance, one may use the spherical variables (2.35) to write

$$\frac{\delta W}{\delta \Pi} = 0 = \frac{\delta W}{\delta \Phi}, \quad (5.1)$$

which are the static versions of the Hamilton equations (2.36). In this section, we shall neither write out nor solve the above equations explicitly but merely use them to derive some general relations.

For the moment, let us ignore the film boundaries and assume that the medium extends to infinity in all directions. We may then apply Derrick's scaling argument in a straightforward fashion. Suppose that $\Pi = \Pi(\mathbf{x})$ and $\Phi = \Phi(\mathbf{x})$ is a solution of Eqs. (5.1) with (finite) energy $W = W_e + W_a + W_b + W_m$. The energy of the configuration $\Pi(\zeta\mathbf{x})$ and $\Phi(\zeta\mathbf{x})$, where ζ is some constant, is then given by

$$W(\zeta) = \frac{1}{\zeta} W_e + \frac{1}{\zeta^3} (W_a + W_b + W_m). \quad (5.2)$$

By our hypothesis $\zeta = 1$ is a stationary point of $W(\zeta)$ and hence $W'(\zeta = 1) = 0$ or

$$W_e + 3(W_a + W_b + W_m) = 0, \quad (5.3)$$

which is a virial relation that must be satisfied by any static solution with finite energy. Since all pieces of the energy are positive definite, one must conclude from Eq. (5.3) that nontrivial static solutions with finite energy do not exist in a 3D ferromagnetic continuum without boundaries.

The preceding derivation of virial relation (5.2) is clearly inapplicable in the presence of boundaries. We thus seek to obtain the analog of this relation for the film geometry of Fig. 1 by a method that was already employed in the simpler context of Ref. [4] and leads to a series of virial theorems, Derrick’s relation being the simplest example. An alternative form of the Thiele force density is given by

$$\tau_k = \frac{\delta W}{\delta \Pi} \partial_k \Pi + \frac{\delta W}{\delta \Phi} \partial_k \Phi = \partial_l \sigma_{kl} \quad (5.4)$$

and vanishes for static solutions satisfying Eqs. (5.1). Therefore the stress tensor satisfies the continuity equation

$$\partial_l \sigma_{kl} = 0 \quad (5.5)$$

within the ferromagnetic medium. Recalling that the stress tensor satisfies the continuity equation outside the film even for time-dependent solutions, see Eq. (3.22), we conclude that static solutions satisfy Eq. (5.5) everywhere.

A series of virial relations may now be derived by taking suitable moments of Eq. (5.5) and by a systematic application of the divergence theorem. The simplest possibility is

$$\int_V x_j \partial_l \sigma_{kl} dV = 0, \quad (5.6)$$

where the integration extends over some volume V that is left unspecified for the moment. The divergence theorem then yields

$$\int_V \sigma_{ij} dV = \oint_S x_j \sigma_{il} dS_l, \quad (5.7)$$

where we have effected a trivial rearrangement of indices and S is the surface surrounding the volume V . It is understood that the region of integration is such that the surface S does not cross the film boundaries because of potential discontinuities that may render the divergence theorem invalid.

Thus we proceed with an application of Eq. (5.7) in several steps. First we consider the subset of relations obtained by restricting the indices i and j to the values 1 or 2. Using our standard convention we write

$$\int_V \sigma_{\mu\nu} dV = \oint_S x_\nu \sigma_{\mu l} dS_l, \quad (5.8)$$

where $\mu, \nu = 1$ or 2 , and subsequently apply this relation to each region I, II or III separately:

$$\begin{aligned} \int_I \sigma_{\mu\nu} dV &= S_{\mu\nu}^+ - S_{\mu\nu}^-, \\ \int_{II} \sigma_{\mu\nu} dV &= -S_{\mu\nu}^+, \\ \int_{III} \sigma_{\mu\nu} dV &= S_{\mu\nu}^-, \end{aligned} \quad (5.9)$$

where

$$\begin{aligned} S_{\mu\nu}^\pm &\equiv \int_{x_3=\pm d/2} x_\nu \sigma_{\mu 3} dx_1 dx_2 \\ &= \int_{x_3=\pm d/2} x_\nu h_\mu b_3 dx_1 dx_2. \end{aligned} \quad (5.10)$$

Here we have recalled the boundary values of the tensor elements $\sigma_{\mu 3}$ from Eq. (4.8) which are continuous across each boundary for $\mu = 1$ or 2 . In fact, the last two equations in (5.9) coincide with Eqs. (4.14) and (4.15) obtained in our earlier discussion of conservation laws because the stress tensor satisfies the continuity equation outside the film even for time-dependent fields. However the first equation in (5.9) applies only to static solutions. An immediate consequence of all three equations is the set of relations

$$\int_{\text{all volume}} \sigma_{\mu\nu} dV = 0, \quad \mu, \nu = 1 \text{ or } 2, \quad (5.11)$$

where explicit surface contributions are no longer present. A special case that emphasizes the role of the magnetostatic interaction is obtained by contracting both sides of Eq. (5.11) with the 2D antisymmetric tensor,

$$\int \varepsilon_{\nu\mu} \sigma_{\mu\nu} dV = \int (m_1 h_2 - m_2 h_1) dV = 0, \quad (5.12)$$

a relation that is consistent with Eqs. (4.19) and (4.23) since both the orbital angular momentum l and the total magnetic moment μ are time independent in a static solution.

The absence of explicit surface terms in Eq. (5.11) is not surprising because scaling arguments of the Derrick variety continue to apply in the x_1 and x_2 directions. Specifically Eq. (5.11) may be arrived at also by performing the linear transformation $x_1 \rightarrow \zeta_{11}x_1 + \zeta_{12}x_2$ and $x_2 \rightarrow \zeta_{21}x_1 + \zeta_{22}x_2$ in a static solution and by demanding that the resulting energy $W = W(\zeta)$ be stationary at $\zeta_{11} = 1 = \zeta_{22}$ and $\zeta_{12} = 0 = \zeta_{21}$. However the situation is different when one or both indices i, j in Eq. (5.7) are equal to 3.

Actually some useful information on the latter case can be obtained directly from the continuity equation (5.5) which is written as

$$\partial_\nu \sigma_{i\nu} + \partial_3 \sigma_{i3} = 0 \quad (5.13)$$

and implies that the double integrals $\int \sigma_{i3} dx_1 dx_2$, with $i = 1, 2$ or 3 , are independent of x_3 but may assume different values in regions I, II, or III. In fact, all integrals vanish outside the film because they can be calculated at large $|x_3|$ where the tensor elements vanish. For $i = \mu = 1$ or 2 the integrals vanish also inside the film thanks to Eq. (4.9):

$$\int \sigma_{\mu 3} dx_1 dx_2 = 0, \quad \mu = 1 \text{ or } 2, \quad (5.14)$$

for any x_3 . On the other hand,

$$\int \sigma_{33} dx_1 dx_2 = \begin{cases} 0, & |x_3| > \frac{1}{2}d \\ s, & -\frac{1}{2}d < x_3 < \frac{1}{2}d \end{cases} \quad (5.15)$$

where s is constant throughout the film but need not vanish. Collecting the above information we may also write

$$\int_{\text{all volume}} \sigma_{33} dV = sd, \quad (5.16)$$

which should be contrasted with Eq. (5.11) where the right-hand side vanishes.

We have thus derived a number of virial relations that must be satisfied by any static solution. We have also gathered sufficient information to make contact with relation (5.3) obtained for a strictly 3D medium. Indeed Eqs. (5.11) and (5.16) may be combined to yield

$$\int \text{tr } \sigma dV = sd, \quad (5.17)$$

where the integration extends over all volume, $\text{tr } \sigma = \sigma_{11} + \sigma_{22} + \sigma_{33}$ is the trace of the stress tensor, s the constant defined from Eq. (5.15), and d the film thickness. The trace is calculated by using the explicit expression of the stress tensor from Eqs. (3.18) and (3.19):

$$\text{tr } \sigma = w_e + 3(w_a + w_b) + (\mathbf{h} \cdot \mathbf{b}) - \frac{3}{2}\mathbf{b}^2, \quad (5.18)$$

where w_e, w_a and w_b are the exchange, anisotropy and bias energy densities. We may further insert in Eq. (5.18) the magnetic induction $\mathbf{b} = \mathbf{h} + \mathbf{m}$ to write

$$\text{tr } \sigma = w_e + 3(w_a + w_b) - \frac{1}{2}\mathbf{h}^2 + 4\left(-\frac{1}{2}\mathbf{h} \cdot \mathbf{m}\right) - \frac{3}{2}\mathbf{m}^2, \quad (5.19)$$

where the magnetostatic energy density appears both in the form entering Eq. (2.25) and that of Eq. (2.32), while in the last term set $\mathbf{m}^2 = 1$ within the film and zero outside. Therefore a more explicit form of Eq. (5.17) reads

$$W_e + 3[W_a + W_b + (W_m - W_m^{(0)})] = sd, \quad (5.20)$$

where we recognize the various pieces of the energy, as in relation (5.3), and $W_m^{(0)}$ originates in the last term of Eq. (5.19) and is equal to the magnetostatic energy of the ground state configuration $\mathbf{m}_0 = (0, 0, 1)$.

Virial relation (5.20) differs from (5.3) in two significant ways. First, a surface term appears in the right-hand side which is entirely due to the film geometry and is generally different from zero. Second, the magnetostatic energy of the ground state, $W_m^{(0)}$, is subtracted out. Now implicit in the derivation of (5.3) was the assumption that the magnetostatic field vanishes at large distances, in all directions, so that the energy W_m is finite. This assumption is clearly false in a ferromagnetic film because $\mathbf{h} = -\mathbf{m}_0$ at large x_1 and x_2 and thus both W_m and $W_m^{(0)}$ are infinite. Nevertheless the difference $W_m - W_m^{(0)}$ is expected to be finite for reasonable solutions. Furthermore this difference is no longer positive definite and is, in fact, negative in the case of magnetic bubbles. Indeed the magnetostatic field favors expansion of a domain with magnetization opposite to that of the ground state, which is balanced by the exchange, anisotropy and bias fields to produce a stable bubble of definite radius [19]. Therefore virial

relation (5.20), unlike (5.3), does not a priori exclude nontrivial static solutions in a ferromagnetic film, irrespectively of the sign of the surface contribution in the right-hand side. An explicit example is worked out in the following section where both $W_m - W_m^{(0)}$ and s are negative but Eq. (5.20) is verified.

6. The fundamental magnetic bubble

The construction of static solutions with a nonvanishing winding number is an issue of significant practical interest and occupied most of the early studies of magnetic bubbles [2,3]. Because of the long-range nature of the magnetostatic field and the related effects of finite film thickness, writing out the static equations (5.1) explicitly leads to a rather complex system that is not particularly illuminating. Hence the question was addressed through approximate solutions in the limit of a large quality factor κ [19], variational methods [20], and numerical simulations in the important special case of the fundamental ($Q = 1$) bubble [21]. However, in order to illustrate some basic aspects of our theoretical development, we shall need some detailed information on the profile of a bubble that is not easily accessible from the early work. We have thus decided to recalculate the $Q = 1$ bubble by a numerical method with a simple physical origin.

Suppose that some initial configuration with a given winding number Q evolves according to the Landau–Lifshitz equation (2.37) including dissipation. After a sufficiently long time interval precession effects are suppressed and the configuration eventually relaxes to a static solution of the Landau–Lifshitz equation with the same winding number. Since our aim in this section is only to obtain static solutions, the process may be accelerated using Eq. (2.37) with a very large dissipation constant λ . On introducing the rescaled time variable $\tau = t/\lambda$, the $\lambda \rightarrow \infty$ limit of Eq. (2.37) reads

$$\frac{\partial \mathbf{m}}{\partial \tau} + \mathbf{m} \times (\mathbf{m} \times \mathbf{f}) = 0, \quad \mathbf{m}^2 = 1. \quad (6.1)$$

In view of Eq. (2.38) the energy decreases when the configuration evolves according to either Eq. (2.37) or its fully dissipative limit (6.1). The advantage of the

latter is that it suppresses transients and leads to equilibrium with reasonable speed. Of course, the calculated static solution is independent of the details of the initial configuration provided that the winding number is kept fixed. Thus the initial condition may be chosen more or less at convenience and convergence may be improved by incorporating any a priori information on the expected static solution. To be sure, Eq. (6.1) cannot be used as a substitute for the complete Landau–Lifshitz equation but merely as a means to derive a numerical relaxation algorithm for the calculation of static solutions.

Although the principle of the method is very simple, an efficient solution of the initial-value problem posed in the preceding paragraph confronts us with a nontrivial numerical task; at every step of the time evolution one must solve the Poisson equation (2.27) in order to determine the magnetostatic field \mathbf{h} and subsequently the effective field \mathbf{f} from Eq. (2.13). Calculation of the latter near the film boundaries should also take into account the unpinned boundary condition (2.22). A detailed description of our numerical algorithm will be given elsewhere [22], so the remainder of this section will be devoted to a discussion of the results of an explicit calculation of the fundamental magnetic bubble.

A substantial simplification occurs in the case of the fundamental bubble because of its *strict* axial symmetry; that is, *invariance* under a simultaneous rotation in the (x_1, x_2) plane and a corresponding azimuthal rotation of the magnetization. It is then convenient to use cylindrical coordinates defined from

$$x_1 = \rho \cos \phi, \quad x_2 = \rho \sin \phi, \quad x_3 = z. \quad (6.2)$$

A strictly axially symmetric configuration is of the general form

$$m_1 + im_2 = (m_\rho + im_\phi)e^{i\phi}, \quad m_3 = m_z \quad (6.3)$$

where the radial (m_ρ), azimuthal (m_ϕ) and longitudinal (m_z) components are functions of only ρ and z ,

$$\begin{aligned} m_\rho &= m_\rho(\rho, z), \\ m_\phi &= m_\phi(\rho, z), \\ m_z &= m_z(\rho, z), \end{aligned} \quad (6.4)$$

while they continue to satisfy the constraint

$$m_\rho^2 + m_\phi^2 + m_z^2 = 1. \quad (6.5)$$

The dissipative equation (6.1) becomes effectively two-dimensional and a significant simplification of the numerical problem results.

Specifically, when ansatz (6.3) is inserted in Eq. (6.1), the resulting equation retains the same form except that the three-component vector $\mathbf{m} = (m_1, m_2, m_3)$ is formally replaced by (m_ρ, m_ϕ, m_z) and the effective field \mathbf{f} by (f_ρ, f_ϕ, f_z) with

$$\begin{aligned} f_\rho &= \Delta m_\rho - \frac{m_\rho}{\rho^2} - \kappa m_\rho + h_\rho, \\ f_\phi &= \Delta m_\phi - \frac{m_\phi}{\rho^2} - \kappa m_\phi + h_\phi, \\ f_z &= \Delta m_z + h_b + h_z, \end{aligned} \quad (6.6)$$

where the Laplace operator is reduced to

$$\Delta = \frac{\partial^2}{\partial \rho^2} + \frac{1}{\rho} \frac{\partial}{\partial \rho} + \frac{\partial^2}{\partial z^2}, \quad (6.7)$$

h_b is the bias field, and h_ρ, h_ϕ and h_z are the polar components of the magnetostatic field. Actually, the azimuthal component vanishes because

$$\nabla \cdot \mathbf{m} = \frac{\partial m_\rho}{\partial \rho} + \frac{m_\rho}{\rho} + \frac{\partial m_z}{\partial z} \quad (6.8)$$

and hence the magnetostatic potential is a function of only ρ and z ; $\psi = \psi(\rho, z)$. Therefore

$$h_\rho = -\frac{\partial \psi}{\partial \rho}, \quad h_\phi = 0, \quad h_z = -\frac{\partial \psi}{\partial z}, \quad (6.9)$$

and the polar components of the magnetic induction are

$$b_\rho = h_\rho + m_\rho, \quad b_\phi = m_\phi, \quad b_z = h_z + m_z. \quad (6.10)$$

For future reference we also quote some discrete symmetries of the reduced system of equations. First, given a static solution of the form (6.4), the configuration

$$m_\rho(\rho, z), \quad -m_\phi(\rho, z), \quad m_z(\rho, z) \quad (6.11)$$

is also a solution. Second, the parity relations

$$\begin{aligned} m_\rho(\rho, z) &= -m_\rho(\rho, -z), \\ m_\phi(\rho, z) &= m_\phi(\rho, -z), \\ m_z(\rho, z) &= m_z(\rho, -z), \\ h_\rho(\rho, z) &= -h_\rho(\rho, -z), \\ h_\phi &= 0, \\ h_z(\rho, z) &= h_z(\rho, -z), \end{aligned} \quad (6.12)$$

are compatible with the evolution equation (6.1). In other words, if Eq. (6.1) is solved with an initial condition satisfying relations (6.12), the resulting static solution will satisfy the same relations.

To complete the description of strictly axially symmetric configurations we return briefly to the conservation laws (4.1) and (4.2). The relevant third component of the vorticity reduces to

$$\gamma_3 = \frac{1}{\rho} \frac{\partial m_z}{\partial \rho}. \quad (6.13)$$

Therefore the winding number calculated from Eq. (3.10) is given by

$$\begin{aligned} Q &= \frac{1}{2} \int_0^\infty \frac{\partial m_z}{\partial \rho} d\rho \\ &= \frac{1}{2} [m_z(\infty, z) - m_z(0, z)] = 1, \end{aligned} \quad (6.14)$$

provided that the magnetization approaches its ground-state value $m_z = 1$ at infinity and the value $m_z = -1$ at the origin. We further note the trivial fact that the moments I_μ vanish and the guiding center coincides with the origin of the coordinate system. Finally the orbital angular momentum is computed from Eqs. (4.2) and (6.3),

$$\begin{aligned} l &= \frac{1}{2} \int_{-d/2}^{d/2} dz \int_0^\infty \frac{\partial m_z}{\partial \rho} 2\pi \rho^2 d\rho \\ &= - \int_{-d/2}^{d/2} dz \int_0^\infty (m_z - 1) 2\pi \rho d\rho, \end{aligned} \quad (6.15)$$

where we have performed a partial integration taking into account that $m_z = 1$ at infinity. We then recognize in the right-hand side of Eq. (6.15) the total magnetic moment μ of Eq. (4.2). Hence $l = -\mu$ and

$$J = l + \mu = 0. \quad (6.16)$$

As expected, the total angular momentum vanishes for a strictly axially symmetric configuration. A related fact is that the radius r calculated from Eq. (4.29) with $\mathbf{R} = 0$ and $l = -\mu$ satisfies the relation

$$\mu = -2\pi dr^2, \quad (6.17)$$

which could also be obtained by considering a crude model of a bubble where the magnetization points toward the north pole, $\mathbf{m} = (0, 0, 1)$, for $\rho > r$ and toward the south pole, $\mathbf{m} = (0, 0, -1)$, for $\rho < r$.

Now, if Eq. (6.1) is solved for an initial condition with strict axial symmetry and winding number $Q = 1$, it will eventually lead to a static solution with the same symmetry and winding number. A simple choice of the initial configuration is given by the two-parameter family

$$m_\rho = 0, \quad m_\phi = \pm \operatorname{sech} u, \quad m_z = \tanh u \quad (6.18)$$

with

$$u = \ln(\rho/\rho_0) + (\rho - \rho_0)/\delta_0, \quad (6.19)$$

which coincides with the variational ansatz employed by DeBonte [20] treating the constants ρ_0 and δ_0 as variational parameters. The constant ρ_0 is the naive radius of the bubble, i.e., the radius at which the third component of the magnetization vanishes, while both ρ_0 and δ_0 provide a measure of the wall width δ_w in a picture where the bubble is viewed as a curved domain wall:

$$\frac{1}{\delta_w} = \left. \frac{du}{d\rho} \right|_{\rho=\rho_0} = \frac{1}{\rho_0} + \frac{1}{\delta_0}. \quad (6.20)$$

On this occasion we recall that the width of an ideal (straight) domain wall in an infinite medium is

$$\Delta_w = \sqrt{\frac{A}{K}} \quad \text{or} \quad \frac{1}{\sqrt{\kappa}} \quad (6.21)$$

in the original or rationalized units, respectively (see Section 2). Needless to say, for our purposes the constants ρ_0 and δ_0 need not be determined variationally because the relaxation algorithm should lead to the true static solution for any choice of these parameters. However convergence may be accelerated when configuration (6.18) is as close as possible to the true bubble.

The description of the initial ansatz is completed noting that the \pm freedom in Eq. (6.18) reflects the discrete symmetry (6.11). The specific choice of sign in m_ϕ will be referred to as the polarity of the bubble, the winding number being the same ($Q = 1$) for either polarity. Finally configuration (6.18) is independent of z and trivially satisfies the parity relations (6.12). Therefore the anticipated static solution will satisfy the same relations, even though it will develop a nontrivial z dependence.

At this point, one must specify the true parameters of the problem, namely the quality factor κ , the bias field h_b and the film thickness d . We have aimed at providing an illustration where the bubble radius is roughly equal to the film thickness and have thus arrived at the specific values (in rationalized units)

$$\kappa = 2, \quad h_b = 0.32, \quad d = 16\Delta_w = 16/\sqrt{\kappa}, \quad (6.22)$$

which belong to a parameter regime that is thought to be ideal for the formation of magnetic bubbles [19]. A possible choice of the parameters in the initial ansatz (6.19) is accordingly given by $\rho_0 = 18\Delta_w$ and $\delta_0 = 1.1\Delta_w$ but it is certainly not unique. We finally mention that in all of the ensuing graphical illustrations of the fundamental bubble we invoke a slight departure from the rationalized physical units introduced in Section 2 and used throughout the theoretical development; distances will now be measured in units of the ideal domain wall width $\Delta_w = 1/\sqrt{\kappa} = 1/\sqrt{2}$ in order to emphasize the wall structure of the calculated bubble. For instance, the film thickness will appear as $d = 16$.

The calculated fundamental magnetic bubble is illustrated in several ways. We mostly describe a $Q = 1$ bubble with positive polarity, originating in the initial ansatz (6.18) with the upper sign in m_ϕ , the results for negative polarity being inferred from the discrete symmetry (6.11). In Fig. 2 we display the dependence of the magnetization on the radial distance ρ at the film center ($z = 0$) and near the upper boundary ($z = \frac{1}{2}d$); the ρ dependence near the lower boundary ($z = -\frac{1}{2}d$) may be obtained from the parity relations (6.12). The corresponding results for the magnetic induction are shown in Fig. 3. One should keep in mind that the magnetostatic field extends beyond the film boundaries,

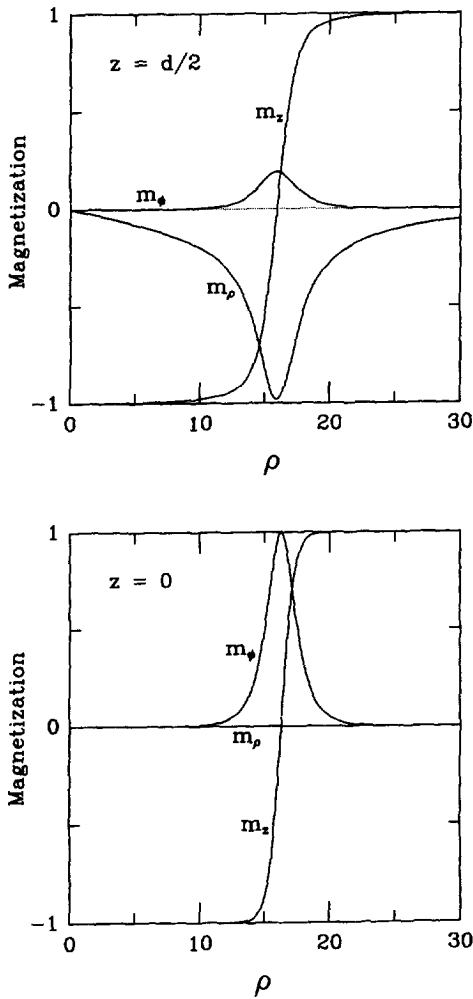


Fig. 2. The calculated magnetization for the fundamental ($Q = 1$) magnetic bubble with positive polarity and parameters specified by Eq. (6.22). Results are given at the film center ($z = 0$) and at the upper boundary ($z = \frac{1}{2}d$), whereas the corresponding results at the lower boundary ($z = -\frac{1}{2}d$) may be inferred from the parity relations (6.12). Here and in all subsequent graphical illustrations distance is measured in units of the ideal wall width $\Delta_w = 1/\sqrt{\kappa}$.

but the calculated values will not be discussed further in the present paper.

Some important general features of the fundamental bubble are already apparent in Fig. 2. If we view the bubble as a curved domain wall, the wall is purely Bloch at the film center ($m_\rho = 0$) and nearly Néel at the boundaries where the radial component m_ρ achieves significant values while the azimuthal com-

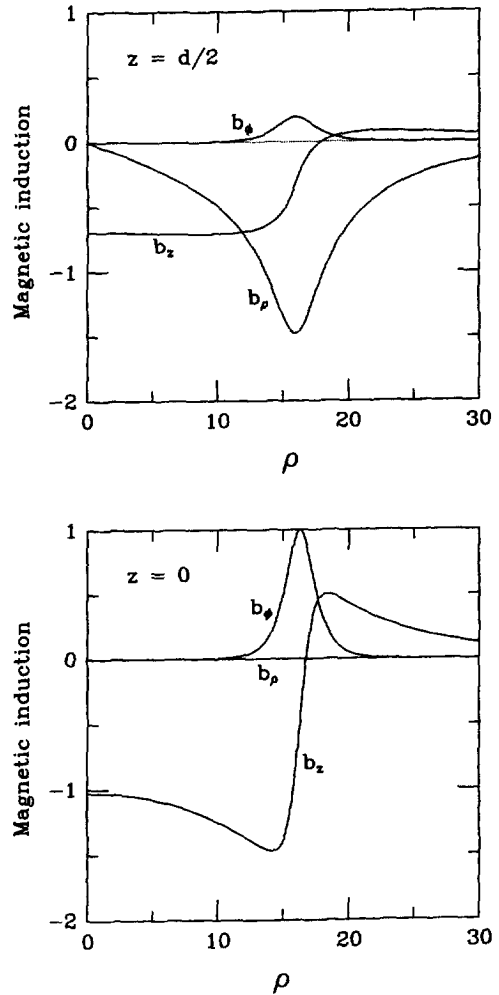


Fig. 3. The calculated magnetic induction for the $Q = 1$ bubble; see caption of Fig. 2 for further explanations.

ponent m_ϕ is small. A better view of the situation is obtained by plotting the projection of the magnetization vector \mathbf{m} on the (x_1, x_2) plane in Fig. 4; whereas Fig. 5 illustrates the projection on a plane that contains the easy axis, which is chosen to be the (x_1, x_3) plane without loss of generality thanks to the axial symmetry.

The case of a $Q = 1$ bubble with negative polarity may be inferred from Eq. (6.11) applied, for example, to Fig. 4. The reflection $m_\phi \rightarrow -m_\phi$ will reverse the sense of circulation of the magnetization at the film center but will not significantly affect the picture at the boundaries where m_ϕ is small.

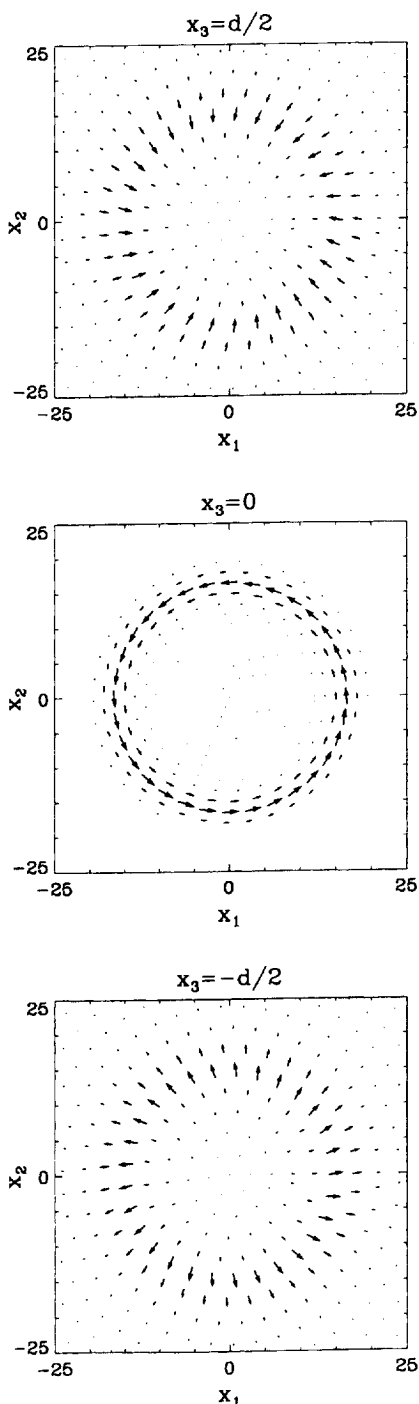


Fig. 4. Illustration of the $Q = 1$ bubble with positive polarity through the projection of the magnetization vector field \mathbf{m} on the (x_1, x_2) plane. The bubble is Bloch-like at the film center ($x_3 = 0$) and Néel-like near the boundaries ($x_3 = \pm \frac{1}{2}d$).

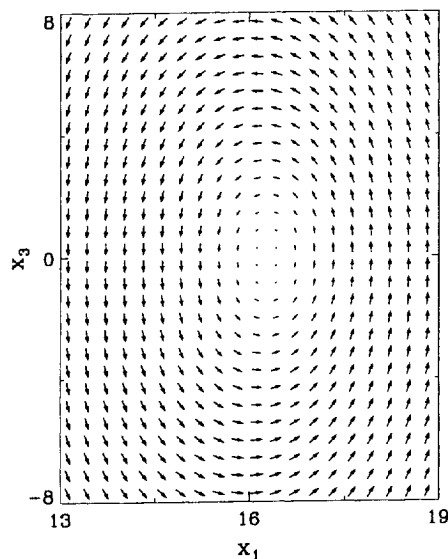


Fig. 5. Another view of the $Q = 1$ bubble through the projection of \mathbf{m} on the (x_1, x_3) plane.

Having thus provided an overall view of the fundamental bubble, we now turn to the description of some important details. The simplest way to analyze the fine structure of the bubble is by recalling the concept of a vortex line introduced in Section 3. We first restate the condition of strict axial symmetry in terms of the spherical variables (2.33):

$$\Theta = \theta(\rho, z), \quad \Phi = \phi + \chi(\rho, z), \quad (6.23)$$

where the function θ and χ are independent of the angle ϕ and are related to the polar components of the magnetization by

$$\cos \theta = m_z, \quad \chi = \arctan(m_\phi/m_\rho). \quad (6.24)$$

Therefore a vortex line is equivalently defined as the intersection of the two surfaces

$$m_z(\rho, z) = m_3, \quad \phi + \chi(\rho, z) = \phi_0, \quad (6.25)$$

where m_3 and ϕ_0 are arbitrary constants in the intervals $[-1, 1]$ and $[0, 2\pi]$, respectively.

The first relation in (6.25) defines a curve in the (ρ, z) plane, illustrated in Fig. 6 for three typical values of m_3 , and the surface obtained by a simple revolution of the curve around the third axis has the shape of a barrel. Of special interest is the case $m_3 = 0$

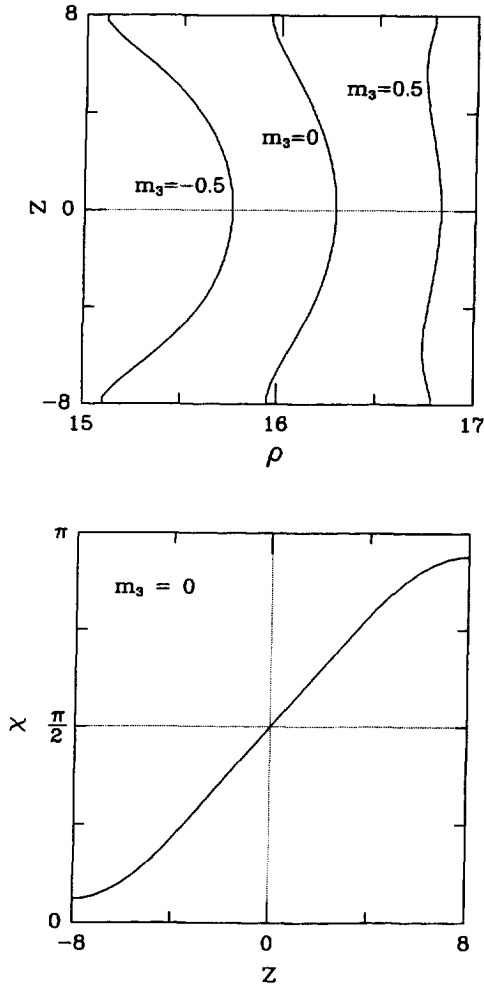


Fig. 6. The calculated curves $m_z(\rho, z) = m_3$ for $m_3 = 0, \pm \frac{1}{2}$ (upper entry) and the z -dependence of χ along a vortex line (lower entry) for the $Q = 1$ bubble with positive polarity; see the text for further explanations.

which may be used to define a (naive) radius of the bubble $\rho_0 = \rho_0(z)$ as the radius of the circular intersection of the barrel with the (x_1, x_2) plane at altitude z . We use the same symbol for the naive radius as for the variational parameter ρ_0 in Eq. (6.19) because the two coincide within the initial ansatz. The current definition of the radius is especially useful at the film boundaries where ρ_0 is the distance from the center of the bubble at which a sharp change in contrast takes place (see Fig. 4) that may be detected experimentally. In our numerical example we found that $\rho_0(z = \pm \frac{1}{2}d) = 15.9\Delta_w$ which should be compared

with the value at the film center $\rho_0(z = 0) = 16.3\Delta_w$, thus providing a measure of bubble bulging [19]. We also quote the average value of the naive radius

$$\bar{\rho}_0 = \frac{1}{d} \int_{-d/2}^{d/2} \rho_0(z) dz = 16.15\Delta_w \quad (6.26)$$

and compare it with the radius r defined by Eq. (4.29) and related to the total magnetic moment by Eq. (6.17):

$$r = 16.21\Delta_w. \quad (6.27)$$

The radius r appears naturally within the theoretical development, as will become evident in the discussion of skew deflection in Section 7, whereas the naive radius ρ_0 is closer to what is actually measured in an experiment. Therefore the observed proximity of the numerical values quoted in Eqs. (6.26) and (6.27) is of special significance. Note incidentally that the calculated bubble radius for the specific parameters (6.22) is approximately equal to the film thickness.

Next we consider the second relation in (6.25). We will not attempt to draw the corresponding surfaces, for various values of the constant ϕ_0 , but examine directly their intersections (vortex lines) with a barrel at given m_3 . Thus in Fig. 6 we also display the z -dependence of χ along a vortex line; that is, we plot the function $\chi(\rho(z; m_3), z) \equiv \chi(z; m_3)$ where $\rho(z; m_3)$ is the root of the algebraic equation $m_z(\rho, z) = m_3$ which depends on z and the particular value of m_3 . At $m_3 = 0$, the root $\rho(z; m_3 = 0)$ reduces to the naive radius $\rho_0(z)$ discussed in the preceding paragraph. Actually Fig. 6 shows the z -dependence of χ along a vortex line only for $m_3 = 0$, but our numerical simulation furnished values for χ that are virtually indistinguishable when m_3 varies in the region $|m_3| \lesssim \frac{1}{2}$. Nevertheless departures from such a universal behavior occur for $|m_3| > \frac{1}{2}$.

The preceding findings are best summarized by the sketch of a typical vortex line given in Fig. 7. Since the sum $\phi + \chi(\rho(z; m_3), z)$ must remain equal to a constant ϕ_0 , a vortex line originating at a point A of the upper boundary, i.e., at given ϕ_0 and m_3 , proceeds downward along the surface of the barrel at the same time twisting by an amount determined by the variation of χ illustrated in the lower part of Fig. 6. The

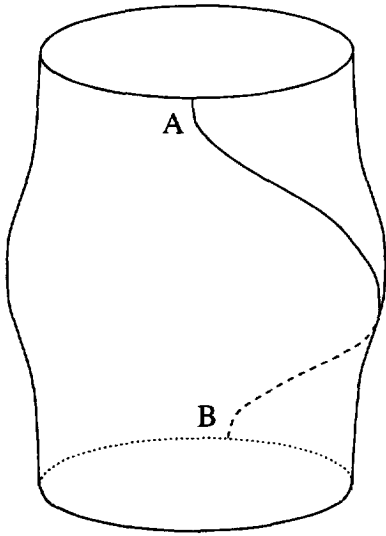


Fig. 7. Sketch of a typical vortex line for a $Q = 1$ bubble with positive polarity. The sense of twist is reversed for a $Q = 1$ bubble with negative polarity.

vortex line eventually terminates at the lower boundary, at a point B , having suffered a total twist $\Delta\phi = -\Delta\chi = -\chi(z = \frac{1}{2}d; m_3) - \chi(z = -\frac{1}{2}d; m_3)$ which generally depends on m_3 . For the specific example $m_3 = 0$ shown in Fig. 6 the calculated total twist is $\Delta\phi = 158^\circ$. This value remains practically the same in the range $|m_3| \lesssim \frac{1}{2}$ but deviations do occur for $|m_3| > \frac{1}{2}$. Finally we note that the vortex lines twist around the surface of a barrel counter-clockwise for the $Q = 1$ bubble with positive polarity considered in our illustrations; the twist take place clockwise for the $Q = 1$ bubble with negative polarity obtained through the discrete symmetry (6.11).

Returning to the topological classification discussed in Section 3, we note that all vortex lines in the fundamental magnetic bubble terminate at the film boundaries and do not tangle with each other. Hence a definition of a Hopf index is not possible, as expected for a film of finite thickness. On the other hand, the flux of vorticity through the plane (x_1, x_2) is equal to 4π for all z , thus leading to a unit winding number.

We also return to the virial relations derived in Section 5 and comment on the manner they are satisfied in our explicit calculation of the fundamental bubble. Because of the strict axial symmetry the surface inte-

grals $s_{\mu\nu}^\pm$ of Eq. (5.10) reduce to

$$S_{\mu\nu}^\pm = S^\pm \delta_{\mu\nu}, \tag{6.28}$$

where $\delta_{\mu\nu}$ is the 2D Kronecker delta and

$$S^\pm = \frac{1}{2} \int_{x_3=\pm d/2}^{\infty} \rho h_\rho b_z 2\pi\rho d\rho. \tag{6.29}$$

Hence relations (5.9) applied for $\mu \neq \nu$ simplify to

$$\int \sigma_{12} dV = 0 = \int \sigma_{21} dV, \tag{6.30}$$

which are valid in each region I, II or III separately. In fact, using the explicit expression of the stress tensor for an axially symmetric configuration, Eqs. (6.30) reduce to the single equation

$$\int h_\rho m_\phi dV = 0, \tag{6.31}$$

which is automatically satisfied thanks to the parity relations (6.12). Furthermore Eqs. (5.9) applied for $\mu = \nu = 1$ or 2 yield for the various regions

$$\begin{aligned} \int_I \sigma_{11} dV &= \int_I \sigma_{22} dV = S^+ - S^-, \\ \int_{II} \sigma_{11} dV &= \int_{II} \sigma_{22} dV = -S^+, \\ \int_{III} \sigma_{11} dV &= \int_{III} \sigma_{22} dV = S^-, \end{aligned} \tag{6.32}$$

as well as

$$\int \sigma_{11} dV = 0 = \int \sigma_{22} dV, \tag{6.33}$$

when the integration extends over all volume. The above relations were verified explicitly in our numerical simulation and were thus used to test its validity. We further verified the Derrick-like relation (5.20) in our specific numerical example where $W_e = 4134$, $W_a = 6008$, $W_b = 11952$, $W_m - W_m^{(0)} = -22573$, and $sd = -9713$; here energy is measured in the rationalized units introduced in Section 2.

7. Skew deflection

We are thus ready to study the main dynamical question posed in Section 1. A static bubble with winding number Q initially located at, say, the origin of the coordinate system is subjected to an external magnetic field

$$\mathbf{h}_{\text{ext}} = (0, 0, h_{\text{ext}}), \quad h_{\text{ext}} = h_{\text{ext}}(\mathbf{x}, t), \quad (7.1)$$

that points along the easy axis and its strength is some prescribed function of position and time. Our task is to determine the response of the bubble to such an external probe. In the absence of dissipation ($\lambda = 0$) the relevant dynamical equation is Eq. (2.15) extended according to

$$\mathbf{f} \rightarrow \mathbf{f} + \mathbf{h}_{\text{ext}}, \quad (7.2)$$

in order to include the effect of the applied field (7.1) which is turned on at $t = 0$. One must then solve the resulting equation with an initial condition provided by the static bubble and calculate the magnetization $\mathbf{m} = \mathbf{m}(\mathbf{x}, t)$ at all later times.

However a great deal can be learned without actually solving this initial-value problem thanks to the special nature of the conservation laws derived in Section 4. Since the position of the guiding center $\mathbf{R} = (R_1, R_2)$ is conserved in the absence of dissipation and external fields other than a uniform bias field, examining the rate at which \mathbf{R} changes in the presence of the field (7.1) should yield direct information on the response of the bubble. The vorticity γ now obeys the relation

$$\dot{\gamma}_i = \varepsilon_{ijk} [\partial_j \partial_l \sigma_{kl} - \partial_j (\mathbf{h}_{\text{ext}} \cdot \partial_k \mathbf{m})], \quad (7.3)$$

which is Eq. (3.11) or (3.15) extended according to Eq. (7.2). In particular, the evolution of the third component of the vorticity is governed by

$$\dot{\gamma}_3 = \varepsilon_{\nu\lambda} [\partial_\nu \partial_l \sigma_{\lambda l} - \partial_\nu (\mathbf{h}_{\text{ext}} \cdot \partial_\lambda \mathbf{m})], \quad (7.4)$$

where we have returned to the 2D notation for Greek indices, as in Section 4, except for the index l that is summed over all three values. The evolution of the moments I_μ of Eq. (4.1) is then given by

$$\dot{I}_\mu = \int \varepsilon_{\nu\lambda} x_\mu [\partial_\nu \partial_l \sigma_{\lambda l} - \partial_\nu (\mathbf{h}_{\text{ext}} \cdot \partial_\lambda \mathbf{m})] dV, \quad (7.5)$$

where the contribution of the first term may be shown to vanish by reasoning completely analogous to that used in the derivation of the conservation laws in Section 4. Implicit in the above statement is the assumption that the applied field does not affect significantly the configuration of the bubble at large distances or, equivalently, it does not affect the ground state of the ferromagnet. We shall return to this assumption later in this section. Thus the evolution of the moments in the presence of the applied field is governed by

$$\begin{aligned} \dot{I}_\mu &= - \int \varepsilon_{\nu\lambda} x_\mu \partial_\nu (h_{\text{ext}} \partial_\lambda m_3) dV \\ &= \int \varepsilon_{\mu\nu} h_{\text{ext}} \partial_\nu m_3 dV, \end{aligned} \quad (7.6)$$

where we have taken into account that the field (7.1) points in the third direction and have also performed an elementary partial integration. On the assumption that $m_3 \rightarrow 1$ sufficiently fast at spatial infinity, one may perform a further partial integration to write

$$\dot{I}_\mu = - \int (\varepsilon_{\mu\nu} \partial_\nu h_{\text{ext}}) (m_3 - 1) dV. \quad (7.7)$$

Also recall that the winding number is conserved even in the presence of the applied field provided that the latter does not destroy the ground state of the ferromagnet. Therefore the drift velocity of the bubble may be inferred from Eqs. (4.28) and (7.7):

$$V_\mu \equiv \dot{R}_\mu = - \frac{1}{4\pi d Q} \int (\varepsilon_{\mu\nu} \partial_\nu h_{\text{ext}}) (m_3 - 1) dV. \quad (7.8)$$

This result for the drift velocity is not completely explicit because the third component of the magnetization appearing under the integral sign must still be determined through a detailed solution of the initial-value problem described in the introductory paragraphs of this section. However Eq. (7.8) already contains the essential information concerning the experimentally observed skew deflection of magnetic bubbles, for it suggests that the drift velocity will acquire a significant component mainly in a direction perpendicular to the gradient of the applied field.

In order to appreciate the physical content of Eq. (7.8) the applied field is written as

$$h_{\text{ext}} = gx_1, \quad g = g(x, t), \quad (7.9)$$

where the “gradient” g may still be a function of position and time. The two components of the drift velocity (7.8) are given equivalently by

$$\begin{aligned} V_1 &= -\frac{1}{4\pi dQ} \int (x_1 \partial_2 g)(m_3 - 1) dV, \\ V_2 &= \frac{1}{4\pi dQ} \int (g + x_1 \partial_1 g)(m_3 - 1) dV \end{aligned} \quad (7.10)$$

The field is now restricted to the physically interesting situation where the gradient is nearly spatially uniform, i.e. $g \approx g(t)$, over a large region surrounding the bubble and drops to zero outside that region. Under such conditions all implicit assumptions made in deriving Eqs. (7.10) are satisfied. In particular, all partial integrations performed on the assumption that the field does not significantly alter the behavior of the bubble at large distances are justified. Nevertheless it is clear from Eqs. (7.10) that an especially transparent result would be obtained in the ideal limit where the gradient g is spatially uniform everywhere. Then

$$g = g(t); \quad V_1 = 0, \quad V_2 = \frac{\mu g}{4\pi dQ}, \quad (7.11)$$

where μ is the total magnetic moment defined in Eq. (4.2).

A completely uniform gradient would imply an infinite field at $x_1 \rightarrow -\infty$ opposing the magnetization in its ground state $\mathbf{m} = (0, 0, 1)$. Therefore, in the presence of some dissipation, the magnetization would align with the applied field almost immediately after the field is turned on and assume the value $\mathbf{m} = (0, 0, -1)$ far in the left plane. Such an instance would destroy the original topological structure of the bubble and obscure the question of skew deflection. Nevertheless the preceding criticism does not apply in the case of vanishing dissipation considered so far because the magnetization would then precess wildly around the easy axis far in the left plane but never align with the external field. Hence the uniform limit considered in Eq. (7.11) is mathematically meaningful in the absence of dissipation and provides the clearest, albeit idealized, illustration of the main theme discussed in this paper.

The guiding center of a bubble with $Q \neq 0$ moves in a direction perpendicular to the applied gradient, in analogy with the familiar Hall motion of an electric charge in a uniform magnetic field (the analog of the winding number) and a uniform electric field (the analog of the uniform magnetic-field gradient). Furthermore the drift velocity (7.11) is expressed in terms of quantities with a simple physical meaning. However this expression for the drift velocity is not completely explicit because the total moment is not conserved during the application of the gradient and thus acquires some time dependence $\mu = \mu(t)$ that can be determined only through a detailed solution of the initial-value problem. The moment μ would be conserved if the magnetostatic field were absent. Indeed the orbital angular momentum l and the total magnetic moment μ would then be separately conserved in the absence of the applied field and, while the latter violates conservation of l because it breaks rotational symmetry, it does not affect μ because it points in the third direction. Under such conditions Eq. (7.11) provides an explicit expression for the drift velocity since the conserved moment μ could then be calculated from the initial configuration of the (static) bubble. This situation occurs in the case of the 2D isotropic Heisenberg model where an analytical result for the drift velocity was given in Ref. [4] and was later verified by a numerical simulation in Ref. [5].

Returning to the realistic case where the magnetostatic field is not negligible, we note that the total moment μ may still be calculated from the profile of the static bubble during the initial stages of the process. If we further restrict our attention to the fundamental bubble calculated in Section 6, the moment is related to the bubble radius through Eq. (6.17) and the initial drift velocity may be written as

$$Q = 1; \quad V_1 = 0, \quad V_2 = -\frac{1}{2}gr^2, \quad (7.12)$$

where we may substitute the numerical value for the bubble radius given in Eq. (6.27) which is approximately equal to the naive radius measured in an experiment. Now applying Eq. (7.12) for speed $V = |V_2|$ yields

$$gr^2/2V = 1, \quad (7.13)$$

which is golden rule (1.1) with a deflection angle $\delta = 90^\circ$, as is appropriate in the absence of dissipation, and a winding number $Q = 1$.

One should keep in mind that the above result provides only a partial verification of the golden rule for two reasons. First, Eq. (7.13) is in general violated during the late stages of the process because neither μ nor r are conserved; in particular, the relation $\mu = -2\pi dr^2$ is strictly valid only for a static bubble. Second, one must examine the extent to which (1.1) is valid in the presence of dissipation when the deflection angle is no longer equal to 90° . The last statement follows from the simple physical fact that dissipation induces a tendency for alignment of the magnetization with the external field, which drives the bubble also toward the left half plane where the field points along the negative third direction.

In order to study the effect of dissipation more precisely we return to Eq. (2.37) and extend it according to Eq. (7.2) to write

$$\dot{\mathbf{m}} + (\mathbf{m} \times \mathbf{G}) = 0, \quad \mathbf{m}^2 = 1, \quad (7.14)$$

where the effective field \mathbf{G} is given by

$$\mathbf{G} = \lambda_1(\mathbf{f} + \mathbf{h}_{\text{ext}}) + \lambda_2[\mathbf{m} \times (\mathbf{f} + \mathbf{h}_{\text{ext}})],$$

$$\lambda_1 = \frac{1}{1 + \lambda^2}, \quad \lambda_2 = \frac{\lambda}{1 + \lambda^2}. \quad (7.15)$$

Since Eq. (7.14) is formally identical to the dissipationless equation, with the replacement $\mathbf{f} \rightarrow \mathbf{G}$, the time derivative of the vorticity may be inferred from Eq. (3.11) with the same replacement:

$$\dot{\gamma}_i = -\varepsilon_{ijk} \partial_j (\mathbf{G} \cdot \partial_k \mathbf{m}). \quad (7.16)$$

Substitution of the field \mathbf{G} from Eq. (7.15) leads to

$$\dot{\gamma}_i = \varepsilon_{ijk} \partial_j \{ \lambda_1 \partial_l \sigma_{kl} - \lambda_1 (\mathbf{h}_{\text{ext}} \cdot \partial_k \mathbf{m}) - \lambda_2 [\mathbf{m} \times (\mathbf{f} + \mathbf{h}_{\text{ext}})] \cdot \partial_k \mathbf{m} \}, \quad (7.17)$$

a result that may be used to study the time evolution of the guiding center in a manner analogous to our earlier discussion in the absence of dissipation. The drift velocity is now given by

$$V_\mu = \frac{\varepsilon_{\mu\nu}}{4\pi d Q} \int [\lambda_1 \mathbf{h}_{\text{ext}} + \lambda_2 [\mathbf{m} \times (\mathbf{f} + \mathbf{h}_{\text{ext}})]] \cdot \partial_\nu \mathbf{m} dV, \quad (7.18)$$

which reduces to Eq. (7.8) at vanishing dissipation.

The above result is highly implicit in that the magnetization in the right-hand side must still be determined through a detailed solution of the initial-value problem. However some explicit information can be extracted from Eq. (7.18) for the early stages of the bubble motion. The magnetization may then be calculated from the static profile of the bubble for which $\mathbf{m} \times \mathbf{f} = 0$. Therefore the initial drift velocity is given by

$$V_\mu = \frac{\varepsilon_{\mu\nu}}{4\pi d Q} \int [\lambda_1 \mathbf{h}_{\text{ext}} + \lambda_2 (\mathbf{m} \times \mathbf{h}_{\text{ext}})] \cdot \partial_\nu \mathbf{m} dV, \quad (7.19)$$

where it is understood that the magnetization is that of a static bubble with winding number Q . Taking into account that the field points in the third direction and performing a partial integration in the first term yields the equivalent relation

$$V_\mu = -\frac{\varepsilon_{\mu\nu}}{4\pi d Q} \int [\lambda_1 (\partial_\nu h_{\text{ext}}) (m_3 - 1) + \lambda_2 h_{\text{ext}} (m_1 \partial_\nu m_2 - m_2 \partial_\nu m_1)] dV. \quad (7.20)$$

At this point, one should recall the assumptions on the gradient $g = g(x, t)$ discussed following Eq. (7.9) which are especially important in the presence of dissipation. Specifically the gradient must vanish outside a large region surrounding the bubble, for otherwise both the ground state and the topological structure of the bubble would be significantly altered. Yet the specific choice of the gradient at large distance will certainly affect the long-time behavior of the bubble but should not be crucial during the early motion. Therefore it is still meaningful to approximate the *initial* drift velocity by inserting in Eq. (7.20) the applied field $h_{\text{ext}} = gx_1$ with a gradient $g = g(t)$ that is spatially uniform. If we further restrict Eq. (7.20) to the fundamental magnetic bubble calculated in Section 6 we find that

$$Q = 1; \quad V_1 = -\lambda_2 \frac{g\nu}{4\pi d}, \quad V_2 = \lambda_1 \frac{g(\mu + \lambda c)}{4\pi d}, \quad (7.21)$$

where λ is the dissipation constant, d is the film thickness, and the constants μ , ν and c are given by

$$\begin{aligned}\mu &= \int (m_z - 1) dV, & \nu &= \frac{1}{2} \int (m_\rho^2 + m_\phi^2) dV, \\ c &= \frac{1}{2} \int \rho \left(m_\rho \frac{\partial m_\phi}{\partial \rho} - \frac{\partial m_\rho}{\partial \rho} m_\phi \right) dV.\end{aligned}\quad (7.22)$$

Here μ is the total moment, ν is essentially the anisotropy energy, and c vanishes on account of the parity relation (6.12). Therefore our final result for the initial drift velocity in the presence of dissipation is

$$V_1 = -\lambda_2 \frac{g\nu}{4\pi d}, \quad V_2 = \lambda_1 \frac{g\mu}{4\pi d}. \quad (7.23)$$

Since the total moment μ is always negative and the constant ν positive, the guiding center moves off in the lower left plane with an initial deflection angle δ with respect to the negative x_1 axis given by

$$\tan \delta = \frac{V_2}{V_1} = \frac{1}{\eta\lambda} \quad \text{or} \quad \sin \delta = \frac{1}{\sqrt{1 + \eta^2\lambda^2}}, \quad (7.24)$$

where the coefficient

$$\eta = -\frac{\nu}{\mu} = 0.08 \quad (7.25)$$

is calculated from Eqs. (7.22) using as input the static bubble. The specific numerical value quoted above corresponds to the specific choice of parameters made in Section 6. Finally we calculate the speed

$$V = \sqrt{V_1^2 + V_2^2} = \frac{\sqrt{1 + \eta^2\lambda^2}}{1 + \lambda^2} \frac{g|\mu|}{4\pi d} \quad (7.26)$$

and relate it to the bubble radius through Eq. (6.17) and the deflection angle through Eq. (7.24):

$$\frac{gr^2}{2V} \sin \delta = \frac{1 + \lambda^2}{1 + \eta^2\lambda^2}. \quad (7.27)$$

At vanishing dissipation ($\lambda = 0$) the deflection angle (7.24) becomes $\delta = 90^\circ$ and relation (7.27) reduces to (7.13).

Relation (7.27) establishes contact with the semi-empirical golden rule (1.1) in the important special case of the fundamental magnetic bubble. For small values of the dissipation constant λ encountered in practice [2] the right-hand side of Eq. (7.27) is well approximated by unity, to within terms of order λ^2 , and is thus consistent with Eq. (1.1) applied for $Q = 1$. However this is again only a partial verification of the golden rule because Eq. (7.27) is strictly valid

only for the initial drift velocity. A complete verification would require first to ascertain that the bubble eventually reaches a steady state, namely a state with constant velocity and radius. Such a question could be addressed by a direct numerical solution of the initial-value problem posed in the first paragraph of this section. This numerical task in several respects similar to the solution of the fully dissipative equation (6.1) described in Section 6, except for a technical difference that might prove crucial in practice. Because the applied field breaks rotational invariance the bubble loses its strict axial symmetry during skew deflection and thus leads to a 3D numerical simulation that is beyond our current capabilities.

Nevertheless the question was addressed and answered within a strictly 2D Skyrme model [6] which also leads to Eqs. (7.24) and (7.27) for the initial drift velocity. It was then found through an explicit numerical solution of the initial-value problem that a sharp transient period exists during which the deflection angle departs rapidly and significantly from Eq. (7.24). The transient period is followed by an intermediate regime where the deflection angle reaches a more or less constant value and the golden rule is verified in a rough manner. But a true steady state is never achieved and the finer predictions of the golden rule are not sustained. In particular, the long-time behavior of the bubble is sensitive to the details of the gradient at large distances.

The results from the 2D Skyrme model [6] could be used as a guide for future numerical investigations of the realistic quasi-2D model studied in the present paper. We thus turn to a summary of our main conclusions given in the following section.

8. Concluding remarks

We believe to have provided a clear illustration of an important link that exists between the topological complexity of ferromagnetic structures and their dynamics. The most direct manifestation of such a link is the construction of unambiguous conservation laws as moments of the topological vorticity. The special dynamical features of magnetic bubbles become

transparent and are formally related to more familiar situations such as the Hall effect of electrodynamics or the Magnus effect of fluid dynamics.

Our work has also revealed that some of the quantitative predictions of the early studies must be interpreted with caution. In particular, the golden rule is valid in its gross features but not in its details. Hence there exists room for further development of the dynamical theory of magnetic bubbles. Numerical simulations along the lines of those performed within the strictly 2D Skyrme model [6] could prove feasible and provide important hints concerning the remaining questions. There has also been some speculation to the effect that the dynamics might simplify for hard ($|Q| \gg 1$) bubbles, in analogy with the adiabatic dynamics of electric charges in strong magnetic field fields [5]. The semi-empirical golden rule might then prove to be exact in the extreme large- Q limit and could possibly be corrected through a systematic adiabatic perturbation theory at finite Q .

In this paper we have confined our attention to the response of a bubble to an externally applied magnetic-field gradient. However a field gradient is intrinsically present also in the problem of two or more interacting magnetic bubbles. Thus two interacting bubbles with winding numbers of the same sign are expected to orbit around each other, in analogy with the 2D motion of two electrons in a uniform magnetic field or two vortices in an ordinary fluid. Similarly two bubbles with opposite winding numbers (e.g., $Q = 1$ and $Q = -1$) should move in formation along roughly parallel lines, also in analogy with an electron–positron pair in a uniform magnetic field or a vortex–antivortex pair in a fluid. These expectations were confirmed through numerical simulations in the Skyrme model [6] and should be possible to establish both theoretically and experimentally in real ferromagnetic films. Analogous results are expected for interacting Abrikosov vortices in a superconductor [23].

Finally we return briefly to the possibility of genuinely 3D magnetic solitons alluded to in Section 3. The experimentally observed Bloch points are 3D topological defects whose dynamics has not yet been studied within the present framework. Furthermore theoretical arguments for the existence of magnetic

vortex rings with a nonvanishing Hopf index [4,15] have not yet been concluded to a definite calculation that would provide the necessary background for a corresponding experimental search in the bulk of the ferromagnetic medium.

Acknowledgements

We are grateful to P.J. Lalouis and P.N. Spathis for valuable assistance in the numerical simulation described in Section 6. The work was supported in part by two grants from the EEC(SCI-CT-91-0705 and CHRX-CT93-0332).

References

- [1] A.A. Thiele, Phys. Rev. Lett. 30 (1973) 230; J. Appl. Phys. 45 (1974) 377.
- [2] A.P. Malozemoff and J.C. Slonczewski, Magnetic Domain Walls in Bubble Materials (Academic Press, New York, 1979).
- [3] T.H. O'Dell, Ferromagnetodynamics, the Dynamics of Magnetic Bubbles, Domains and Domain Walls (Wiley, New York, 1981).
- [4] N. Papanicolaou and T.N. Tomaras, Nucl. Phys. B 360 (1991) 425; N. Papanicolaou, in: Singularities in Fluids, Plasmas and Optics, eds. R.E. Caflisch and G.C. Papanicolaou (Kluwer, Amsterdam, 1993) p. 151–158.
- [5] N. Papanicolaou, Physica D 74 (1994) 107; Phys. Lett. A 186 (1994) 119.
- [6] N. Papanicolaou and W.J. Zakrzewski, Physica D 80 (1995) 225; Phys. Lett. A 210 (1996) 328.
- [7] G.H. Derrick, J. Math. Phys. 5 (1964) 1252.
- [8] G.K. Batchelor, An Introduction to Fluid Dynamics (Cambridge University Press, Cambridge 1967).
- [9] H.K. Moffat, J. Fluid Mech. 35 (1969) 117.
- [10] H.K. Moffat, Magnetic Field Generation in Electrically Conducting Fluids (Cambridge University Press, Cambridge, 1978).
- [11] H.K. Moffat, G.M. Zaslavsky, P. Compte and M. Tabor, eds., Topological Aspects of the Dynamics of Fluids and Plasmas, NATO ASI Series (Kluwer, Dordrecht, 1992).
- [12] E.A. Kuznetsov and A.V. Mikhailov, Phys. Lett. A 77 (1980) 37.
- [13] R. Bott and L.W. Tu, Differential Forms in Algebraic Topology (Springer, New York, 1982).
- [14] X.G. Wen and A. Zee, Phys. Rev. Lett. 61 (1988) 1025.
- [15] J.E. Dzyaloshinskii and B.A. Ivanov, JETP Lett. 29 (1979) 540.

- [16] J.C. Slonczewski, *J. Magn. Magn. Mater.* 12 (1979) 108.
- [17] F.D.M. Haldane, *Phys. Rev. Lett.* 57 (1986) 1488.
- [18] G.E. Volovik, *J. Phys. C* 20 (1987) L83.
- [19] A.A. Thiele, *Bell Syst. Tech. J.* 48 (1969) 3287; *J. Appl. Phys.* 41 (1970) 1139.
- [20] W.J. DeBonte *AIP Conf. Proc.* 5 (1971) 140; *J. Appl. Phys.* 44 (1973) 1793; *IEEE Trans. Magn., MAG-11* (1975) 3.
- [21] T.G.W. Blake and E. Della Torre, *J. Appl. Phys.* 50 (1979) 2192; E. Della Torre, C. Hagedüs and G. Kádár, *AIP Conf. Proc.* 29 (1975) 89.
- [22] S. Komineas, Ph.D Thesis, University of Crete.
- [23] N. Papanicolaou and T.N. Tomaras, *Phys. Lett A* 179 (1993) 33.